

VeriSciQA: An Auto-Verified Dataset for Scientific Visual Question Answering

Yuyi Li¹ Daoyuan Chen² Zhen Wang^{1,*} Yutong Lu¹ Yaliang Li^{2,*}

¹Sun Yat-sen University ²Alibaba Group

*Corresponding authors

December 2, 2025

Abstract

Large Vision-Language Models (LVLMs) show promise for scientific applications, yet open-source models still struggle with Scientific Visual Question Answering (SVQA), namely answering questions about figures from scientific papers. A key bottleneck lies in the lack of public, large-scale, high-quality SVQA datasets. Although recent work uses LVLMs to synthesize data at scale, we identify systematic errors in their resulting QA pairs, stemming from LVLMs’ inherent limitations and information asymmetry between figures and text. To address these challenges, we propose a verification-centric *Generate-then-Verify* framework that first generates QA pairs with figure-associated textual context, then applies cross-modal consistency checks against figures along with auxiliary filters to eliminate erroneous pairs. We instantiate this framework to curate VERISCIQA¹, a dataset of 20,351 QA pairs spanning 20 scientific domains and 12 figure types. VERISCIQA poses a challenging benchmark for open-source models, with a substantial accuracy gap between the leading open-source models (64%) and a proprietary model (82%). Moreover, models fine-tuned on VERISCIQA achieve consistent improvements on SVQA benchmarks, with performance gains that scale with data size and surpass models trained on existing datasets. Human evaluation further validates the superior correctness of VERISCIQA. Together, these results demonstrate that continued data expansion by our scalable framework can further advance SVQA capability in the open-source community.

¹Dataset available at <https://huggingface.co/datasets/datajuicer/VeriSciQA>

1 Introduction

Recent advances in Large Vision-Language Models (LVLMs) [1, 3, 23, 27] have unlocked capabilities ranging from everyday image captioning to visually grounded multi-step reasoning. To translate these gains into genuine scientific progress, LVLMs must master a particularly demanding skill: accurately interpreting *scientific figures*, in which authors often condense the core evidence and insights of their studies [31, 39]. Mastering this ability would elevate LVLMs from generic vision-language demonstrators to practical research assistants that can surface results, verify claims, and ultimately accelerate knowledge discovery.

To this end, we focus on the task of *Scientific Visual Question Answering* (SVQA), where an LVLM answers questions grounded in figures from scientific papers. Recent studies [38] show that while proprietary LVLMs are approaching human-level performance, open-source counterparts still lag far behind, struggling with the specialized visual semantics and associated reasoning skills required for interpreting scientific figures. A key contributor to this gap is the absence of a public, large-scale, high-quality SVQA dataset [20, 31], underscoring the need for an automatic approach to synthesize such data that can enhance the capabilities of open-source LVLMs in this domain.

Despite the growing interest in SVQA, existing dataset construction methods face a fundamental trade-off among scalability, diversity, and correctness. Template-based efforts such as FigureQA [16] and SciFiBench [32] achieve scalability but remain constrained by fixed question formats, failing to capture the reasoning variety of the scientific domain. On the other end of the spectrum, manually curated datasets like CharXiv [38] provide high-quality, expert-authored questions but depend on

costly, labor-intensive annotation, limiting both size and domain coverage. Recent approaches, including ArXivQA [20] and SPIQA [31], utilize LVLMs for end-to-end generation, improving scalability and diversity while maintaining reasonable correctness.

Among LVLM-driven generation-only methods, ArXivQA typifies this line of work, and its resulting SVQA dataset has been adopted in some follow-up studies [10, 35, 40]. However, our systematic analysis of its SVQA dataset reveals four recurring categories of erroneous QA pairs (detailed in § 2). Collectively, these errors raise concerns about the reliability of LVLM-driven generation-only methods, highlighting potential risks of fine-tuning LVLMs on their synthesized SVQA datasets.

Furthermore, we identify two primary factors underlying these erroneous QA pairs. Some directly arise from the LVLM’s own deficiencies, consistent with recent findings that even state-of-the-art LVLMs may hallucinate visual content [4]. Others stem from information asymmetry: essential figure-associated context (e.g., the purpose and symbol definitions of the figure) is missing from the model input, while the LVLM’s broad prior knowledge may lead it to generate questions whose answers go beyond what the figure alone conveys. Our observations motivate two key directions for improving SVQA synthesis: First, an effective *verification mechanism* is needed to identify and filter out erroneous QA pairs at scale. Second, *leveraging figure-associated context* from the broader paper content can both improve generation quality and enable more reliable verification by mitigating information asymmetry.

In this paper, we explore and unify the above two directions by proposing a verification-centric *Generate-then-Verify* framework that first leverages figure-associated context for QA generation and then applies a series of verification steps for filtering. Our design builds on the key observation that, in peer-reviewed papers, figure-citing paragraphs are tightly aligned with their accompanying figures, providing a flexible yet reliable signal for factual grounding and some degree of intent alignment. In the first stage of our *Generate-then-Verify* framework, these paragraphs are fed into an LVLM to generate QAs, mitigating figure-intent misalignment. Then cross-modal consistency checks and auxiliary filters are carefully designed to eliminate the remaining three error patterns, without requiring manual intervention.

Our main contributions are as follows:

- **A novel *Generate-then-Verify* framework for SVQA synthesis.** We propose a scalable framework that leverages the cross-modal consistency inherent in peer-reviewed scientific papers

to automatically synthesize VQA data, improving the correctness of generated QA pairs over existing generation-only approaches.

- **A diverse, high-quality, and challenging SVQA dataset.** Built using an instantiation of our proposed framework, VERISCIQA comprises 20,351 QA pairs spanning 20 scientific domains, 12 figure types, and 5 question types. Human evaluation confirms superior quality over existing SVQA datasets. Zero-shot evaluation on our dataset reveals substantial performance gaps between proprietary and open-source models, with both leaving room for improvement.
- **Scaling Data, Scaling Capability.** Models fine-tuned on our dataset achieve consistent improvements across diverse scientific VQA benchmarks, outperforming those trained on existing SVQA datasets. Performance improves as training data scales from 500 to 5,000 examples, reaching +2.28% average gain.

2 Motivation

Among recently proposed SVQA datasets, a typical line relies on LVLM-driven, generation-only methods that prompt a model with a figure from the paper, its accompanying caption, and optional context parsed from the paper’s LaTeX source. ArXivQA [20], a representative dataset in this line, synthesizes more than 100K multiple-choice QA pairs. Despite its large scale, our audit reveals that it still exhibits a substantial error rate, raising concerns about the data quality of such end-to-end generated SVQA datasets [31].

Systematic error analysis of ArXivQA. We randomly sample 100 items from ArXivQA, each released as a five-tuple $\langle \text{Question}, \text{Options}, \text{Label}, \text{Rationale}, \text{Figure} \rangle$, where *Label* refers to the LVLM’s prediction rather than ground truth. Our systematic analysis reveals four common categories of erroneous QA pairs, which we refer to as follows:

- **(E1) Incorrectly Visually Grounded (19/100):** questions or answers that exhibit mismatches between textual claims and the visual evidence [4], e.g., misreading chart values (Fig. 1a).
- **(E2) Figure–Intent Misaligned (7/100):** questions whose semantics diverge from the figure’s purpose, e.g., treating an embedding-space schematic as a natural image and asking for scene classification (Fig. 1b).

- **(E3) Non-Visual** (6/100): answers can be inferred directly from the question and common/domain-specific knowledge, making the figure unnecessary (Fig. 1c).
- **(E4) Outside-Knowledge** (5/100): questions that reference visual elements whose interpretation requires additional context from the paper. Since this context is not included in the question, the question becomes unanswerable (Fig. 1d).

Root causes: hallucination and information asymmetry. LVLMs are known to *hallucinate*, frequently producing responses inconsistent with the visual content provided (i.e., cross-modal inconsistency) [4]. The first two failure modes, E1 and E2, are results of this phenomenon: generation-only methods directly take the model outputs without careful verification, allowing hallucinated responses to pass through. Heuristics such as sampling-based self-consistency or self-checking reduce but cannot eliminate such errors [8, 15, 21, 25, 36]. The other root cause is *information asymmetry*. On the one hand, the input to the LVLm often contains only the figure and its caption, omitting essential figure-associated context (e.g., the figure’s purpose, symbol definitions, or experimental setup) that authors describe in the main body of the paper. Without this context, the model may rely on its broad knowledge to fabricate plausible but unverifiable answers, leading to E2–E4 errors. While large-scale figure–caption resources from arXiv are readily available, there is no community-curated corpus that augments these pairs with the full set of figure-citing paragraphs drawn from across all domains. To address this gap, we enrich caption-only figure inputs with their associated figure-citing paragraphs extracted from the full paper, covering all arXiv domains. Crucially, these paragraphs not only provide missing context but also serve as reliable source material for generating QA pairs.

Key insight: figure-citing paragraphs contain ground-truth claims about figures. Figure-citing paragraphs often contain claims such as “As shown in Fig. 2, accuracy rises by 20%.” about the figure. Such paragraphs can be extracted from the paper’s LaTeX source by matching figure reference commands (e.g., `\cref`). Importantly, generating QA pairs from such claims promotes alignment with the authors’ intended interpretation of the figure, while their verifiability against the figure itself enables a *Generate-then-Verify* framework that systematically mitigates both hallucination and information asymmetry errors (E1–E4).

3 Methodology

To mitigate the four error types (E1–E4) identified in § 2, we propose a *Generate-then-Verify* framework that first generates candidate QA pairs from figure-associated context and then proceeds to a multi-step verification stage.

Fig. 2 illustrates our framework as instantiated to curate VERISCIQA from arXiv papers. Starting from figure-citing paragraphs as figure-associated context, the **Generation** stage (§ 3.2) operates purely on text: we decompose each paragraph into atomic claims and generate a multiple-choice QA pair with plausible distractors only for claims with concrete visual grounding. The **Verification** stage (§ 3.3) then applies cascaded filtering: text-based filtering first ensures source-consistency and visual-dependency without accessing the figure; vision-based filtering then validates each remaining QA candidate against the figure using self-consistency with an LVLm. Only QA pairs that pass all checks are retained in the final dataset. We detail each stage below.

3.1 Framework Formalization

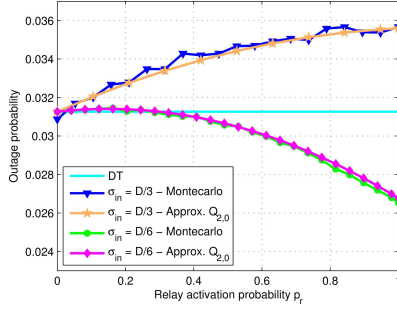
We formalize our framework to provide precise operational definitions that enable reproducibility. Let a scientific paper be represented as $\mathcal{D} = (\mathcal{T}, \mathcal{F})$, where \mathcal{T} is the full text content and $\mathcal{F} = \{(F_i, C_i)\}_{i=1}^N$ is the set of figure-caption pairs. For each figure F_i , we denote its corresponding *figure-associated context* by $\mathcal{P}_i \subset \mathcal{T}$, which consists of paragraph(s) in the document body that explicitly refer to the figure F_i . We process each figure equally and thus omit the index i for brevity.

Let M_{text} denote an LLM and M_{vision} denote an LVLm capable of processing both images and text. In the *Generation* stage, M_{text} extracts a set of atomic claims $\mathcal{S} = \{s_j\}$ from context \mathcal{P} and produces candidate QA pair $q_j = (Q_j, O_j, A_j^*)$ from each claim s_j , where Q_j is the question, O_j is the set of options, and A_j^* is the correct answer. In the *Verification* stage, we apply cascaded filtering with three boolean filters:

$$\begin{aligned} V_{\text{src}} &: (Q, O, A^*, \mathcal{P}) \xrightarrow{M_{\text{text}}} \{\text{True}, \text{False}\} \\ V_{\text{vis_dep}} &: (Q, O, A^*, C) \xrightarrow{M_{\text{vision}}} \{\text{True}, \text{False}\} \\ V_{\text{vis_con}} &: (Q, O, A^*, F, C) \xrightarrow{M_{\text{vision}}} \{\text{True}, \text{False}\} \end{aligned}$$

A candidate q_j is retained in the final dataset if and only if:

$$\begin{aligned} &V_{\text{src}}(Q_j, O_j, A_j^*, \mathcal{P}) \wedge V_{\text{vis_dep}}(Q_j, O_j, A_j^*, C) \\ &\wedge V_{\text{vis_con}}(Q_j, O_j, A_j^*, F, C) = \text{True}. \end{aligned} \quad (1)$$



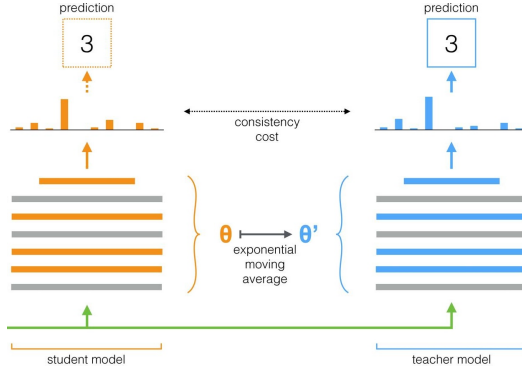
Question: At what relay activation probability does the $\sigma_{in} = D/6$ scenario reach lowest outage?

Options: A. 0.2, B. 0.4, C. 0.6, D. 1.0

Label: C. 0.6

Rationale: The green line shows outage probability decreasing as relay activation increases, reaching the lowest point at around 0.6 before plateauing.

(a) E1: Incorrectly visually grounded



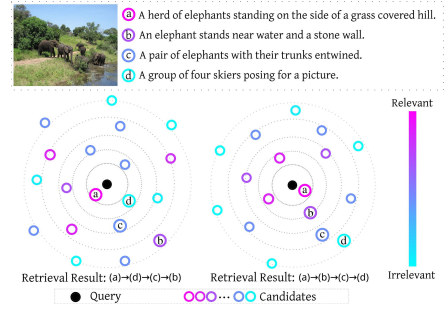
Question: What does "exponential moving average" refer to?

Options: A. Smoothing technique for trends, B. Calculating median values, C. Forecasting stock prices, D. Averaging chemical mixtures

Label: A

Rationale: The 'exponential moving average' is a commonly used technique in time series analysis to smooth out data.

(c) E3: Non-visual



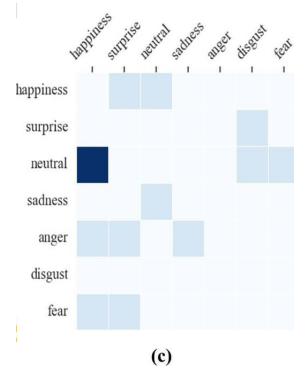
Question: What is the primary subject of the image?

Options: A. Elephants on a hill, B. Elephant near water and wall, C. Elephants with trunks entwined, D. Four skiers posing

Label: B

Rationale: The image shows a single elephant near water with a stone structure. Choices A and C are incorrect because they imply multiple elephants. Choice D is irrelevant as it doesn't feature skiers.

(b) E2: Figure-intent misaligned



Question: Which emotion pair is least likely to co-occur?

Options: A. Happiness-surprise, B. Anger-disgust, C. Sadness-neutral, D. Disgust-fear

Label: D

Rationale: The lightest square is between disgust and fear, suggesting these emotions are least likely to co-occur.

(d) E4: Outside-knowledge

Figure 1: Illustrative examples of the four common error categories (E1–E4).

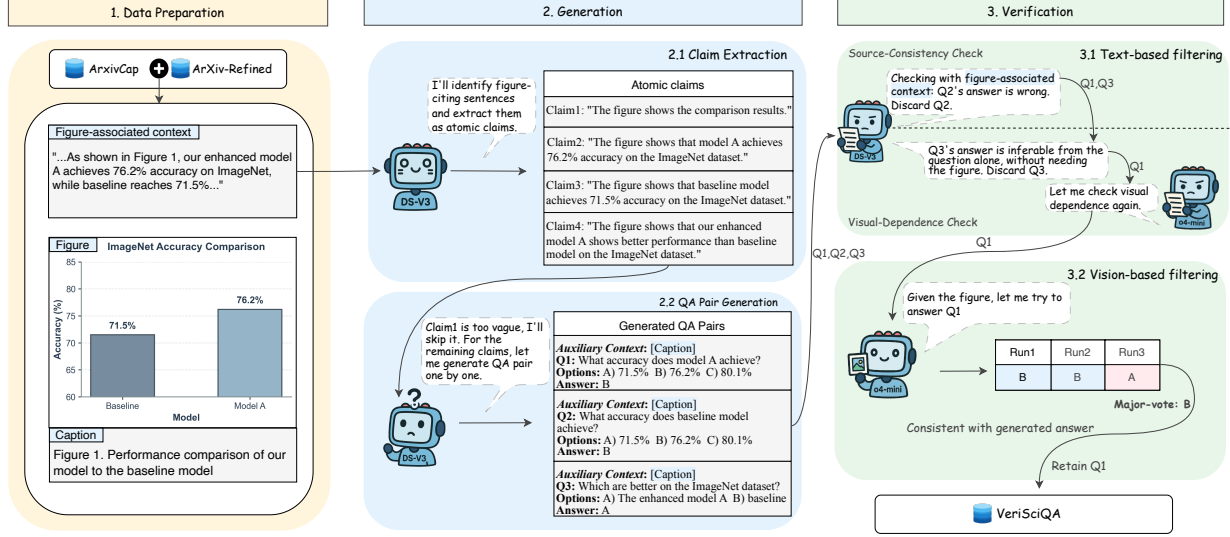


Figure 2: Overview of our Generate-then-Verify framework as instantiated to curate VERISCIQA. We first extract figure-citing paragraphs from arXiv papers as figure-associated context. **Generation** stage then decomposes each context into atomic claims and produces QA pairs only from claims with concrete visual grounding; **Verification** stage applies cascaded text-based and vision-based filtering to remove erroneous candidates.

3.2 Generation

This stage consists of the two steps as follows:

Claim Extraction. We instruct M_{text} to extract and reformulate factual statements about the figure F from \mathcal{P} as atomic claims:

$$\mathcal{S} = \{s_j\} = M_{\text{text}}(\mathcal{P}), \quad (2)$$

where each s_j denotes an atomic claim, a concise, self-contained sentence that asserts what F shows, following the pattern "The figure shows..." (see the illustrative examples in Fig. 2).

QA Pair Generation. For each atomic claim $s_j \in \mathcal{S}$, we further instruct M_{text} to generate a candidate QA pair:

$$q_j = (Q_j, O_j, A_j^*) = M_{\text{text}}(s_j, C, \mathcal{P}), \quad (3)$$

where the model converts s_j into a question Q_j with multiple-choice options O_j (including the correct answer A_j^* and plausible distractors). By generating questions from s_j that explicitly describe what F shows, we ensure figure-intent alignment, mitigating *figure-intent misalignment* errors (E2). M_{text} may decline to produce a QA pair if s_j is too vague or lacks sufficient grounding, e.g., Claim1 in Fig. 2. Each QA pair is retained with its corresponding figure's caption as (C, q_j) , providing additional context to mitigate *outside-knowledge* errors (E4).

3.3 Verification

Each candidate q_j is retained only if it passes all three filters, as defined in Eq. 1. We detail the implementation of each filter below.

Text-Based Filtering. The first step applies two text-only filters without accessing figure F :

- 1. Source-Consistency** **Check**
 $V_{\text{src}}(Q_j, O_j, A_j^*, \mathcal{P})$: We prompt M_{text} to select an answer from O_j given context \mathcal{P} and question Q_j . The filter returns **True** if the model uniquely identifies A_j^* , and **False** otherwise (e.g., when it abstains, selects multiple options, or chooses a different answer; see Q2 dropped by source-consistency check in Fig. 2). This ensures the generated QA pair maintains consistency with the source context.
- 2. Visual-Dependence** **Check**
 $V_{\text{vis-dep}}(Q_j, O_j, A_j^*, C)$: We prompt M_{vision} to select an answer from O_j given only caption C and question Q_j (without figure F). The filter returns **True** if the model fails to identify A_j^* , and **False** otherwise (see Q3 dropped by visual-dependence check in Fig. 2). This ensures that correctly answering this question requires visual information from the figure, thereby mitigating *non-visual* questions (E3).

Vision-Based Filtering. The final step validates

that A_j^* is visually grounded in F and that F and C together provide sufficient information to correctly answer Q_j . While text-based filtering operates purely on textual information, it cannot verify two critical aspects: (i) whether A_j^* is actually supported by visual evidence in F , and (ii) whether the information in F and C is sufficient to answer Q_j without requiring additional context from the paper. Therefore, we design $V_{\text{vis-con}}(Q_j, O_j, A_j^*, F, C)$ so as to prompt M_{vision} to select an answer from O_j based solely on F , C , and Q_j . The filter returns **True** if the model’s prediction matches A_j^* , and **False** otherwise (see Q1 accepted by vision-based filtering in Fig. 2). This eliminates *incorrectly visually grounded* (E1) and *outside-knowledge* (E4) errors. Despite retaining only q_j that M_{vision} answers correctly, the resulting dataset remains challenging (§4.2). Importantly, while this step applies stringent filtering criteria at the cost of dataset quantity, our ablation study (§4.5) confirms that it is essential for ensuring dataset quality.

3.4 Instantiation

We instantiate our framework on scientific figures from peer-reviewed papers in arXiv, leveraging existing datasets and language models to realize each stage.

Data Sources. We combine two complementary data sources: ArXivCap [20], which provides high-quality figure-caption pairs from peer-reviewed papers with heuristic filtering; and RedPajama-ArXiv-Refined [11], which supplies cleaned LaTeX source for extracting figure-associated context. Intersecting these datasets by arXiv ID² yields 572K overlapping papers. We randomly shuffle this pool to avoid temporal or domain-based ordering bias, then process papers in batches until reaching our target dataset size, ultimately processing 44,345 papers.

Context Extraction. For each figure-caption pair (F_i, C_i) , we extract its associated context \mathcal{P}_i by identifying paragraphs that cite F_i via LaTeX reference commands (e.g., `\ref`, `\cref`, or `\autoref`). Details are provided in Appendix A.1.

Model Selection. We use DeepSeek-v3 [22] for M_{text} due to its strong instruction-following capability and wide adoption, and o4-mini [30] for M_{vision} , which achieves strong performance on scientific figure understanding [38]. For the visual-dependence check, to save cost, QA pairs are first filtered by DeepSeek-v3, and only those that pass are further validated by o4-mini (M_{vision}). For vision-based filtering, we prompt M_{vision} to answer the question with

reasoning, querying it three times with stochastic decoding (temperature=1.0) and applying 2-of-3 majority voting to retain only QA pairs where the model consistently selects A^* . For each retained QA pair, we store the reasoning from the first run that agrees with the majority answer; this reasoning is included in the released dataset to enable future applications such as fine-tuning. Prompt templates for all stages are provided in Appendix B.

Resulting Dataset. Applying our Generate-then-Verify framework yields VERISCIQA, a dataset of 20,351 verified multiple-choice QA pairs spanning 20 arXiv categories. Each QA instance consists of a question, multiple-choice options, the correct answer, the associated figure, its caption, and the reasoning generated by M_{vision} . Table 1 shows the filtering statistics at each step.

Table 1: Data filtering statistics at each step.

| Step | Count | Retention |
|------------------------------|---------|-----------|
| Papers | 44,345 | — |
| Atomic claims extracted | 680,877 | 100% |
| QA pairs generated | 261,116 | 38.4% |
| After text-based filtering | 55,372 | 8.1% |
| After vision-based filtering | 20,351 | 3.0% |

The high filtering rates reflect our quality-first design: only 3.0% of atomic claims successfully produce QA pairs that pass the verification stage. Small-scale human evaluation reveals why: in generation, some authors’ claims are too vague or lack sufficient grounding, requiring additional paper content beyond the extracted context to formulate valid QA pairs; in text-based filtering, while providing captions during QA pair generation mitigates *outside-knowledge* errors (E4), this introduces *non-visual* questions (E3) answerable from caption alone; in vision-based filtering, most rejected questions have answers not derivable from the figure, corresponding to *incorrectly visually grounded* (E1) and *outside-knowledge* (E4) errors, though model limitations over-filter a portion of valid instances. Detailed filtering analysis is provided in Appendix D, and further dataset analysis is provided in Section 4.

4 Experiments

We conduct comprehensive experiments to evaluate our dataset from multiple perspectives. We present diversity assessment (§4.1), difficulty assessment through zero-shot evaluation of leading LVLMS (§4.2), and quality comparison with existing SVQA datasets (§4.3). Importantly, we demonstrate that

²The identifier assigned to each arXiv paper (e.g., 2301.12345).

fine-tuning on our dataset yields superior performance over existing SVQA datasets (§4.4), and show consistent performance gains when training on increasing amounts of our data. Finally, we perform ablation studies to validate the contribution of each filtering step (§4.5).

4.1 Diversity Assessment

Our dataset comprises 20,351 diverse QA pairs spanning three key dimensions (Fig. 3): scientific domains, figure types, and question types. Scientific domain labels are assigned according to the arXiv category taxonomy [2] of the source papers, while figure types and question types are automatically annotated using GPT-4o [28]. To verify annotation quality, we randomly sample 50 examples from each category and validate against human annotations, with the reported accuracies (96% for figure types, 86% for question types) representing the minimum accuracy across all categories. Detailed taxonomy definitions and complete distribution tables are provided in Appendix C.

4.2 Difficulty Assessment

We assess dataset difficulty by evaluating leading LVLMS in a zero-shot setting. OpenAI o3 [29] achieves 82.3% overall accuracy, while leading open-source models range from 64–67%, demonstrating that our dataset poses significant challenges with substantial room for improvement across all capability levels. Fig. 4 further decomposes performance across three key dimensions, revealing how different aspects of our dataset pose distinct challenges and expose varying capability levels across models.

Setup. We evaluate four models: OpenAI o3, Qwen2.5-VL (32B/72B)-Instruct [34], and InternVL3-38B [9]. Evaluation is conducted on 1,000 examples stratified by question type, scientific domain, and figure type using zero-shot prompting with greedy decoding. We report accuracy as the evaluation metric. Detailed per-category results are provided in Appendix G.

Results and Analysis. As shown in Fig. 4, we take Qwen2.5-VL-72B as a representative case to analyze the diverse difficulty patterns in detail. Across scientific domains, Astro-Ph (56%) and Physics (59%) present substantial difficulties, demanding specialized domain knowledge and understanding of complex physical phenomena. For figure types, Graph (60%) and Composite figures (63%) are particularly challenging, requiring advanced visual perception skills to understand network structures or inte-

Table 2: Human evaluation results on 100 randomly sampled QA pairs. Ratings on 5-point Likert scale (higher is better).

| Dimension | Rating (1–5) | | | IAA (α) |
|------------------------|--------------|-------|---------|------------------|
| | VERISCIQA | SPIQA | ArxivQA | |
| Factual Correctness | 4.12 | 3.33 | 3.66 | 0.77 |
| Intent Alignment | 4.28 | 4.16 | 3.95 | 0.64 |
| Visual Dependency | 4.78 | 4.26 | 4.66 | 0.78 |
| Self-Containment | 4.20 | 4.17 | 3.72 | 0.74 |
| Overall Quality | 3.98 | 3.24 | 3.21 | 0.75 |

grate information from multiple sub-figures. Among question types, Compositional (62%) and Comparative (63%) questions prove most challenging, requiring multi-step reasoning and cross-element comparison capabilities. These diverse difficulty patterns further reveal that different models exhibit varying strengths: Qwen2.5-VL-32B surpasses its 72B counterpart on several categories, consistent with prior observations [32] that model scale alone does not determine performance on scientific figures. Our dataset’s diverse difficulty landscape helps identify fine-grained capability gaps, providing targeted insights for improvement.

4.3 Quality Comparison

To conduct preliminary verification of data quality, we perform human evaluation on 100 randomly sampled QA pairs (50 from VERISCIQA, 25 from SPIQA [31], 25 from ArxivQA [20]) with 10 annotators (CS graduate students). We assess four quality dimensions corresponding to the error types in §2 on a 5-point Likert scale: Factual Correctness (E1), Intent Alignment (E2), Visual Dependency (E3), and Self-Containment (E4), along with an overall quality rating. As shown in Table 2, our dataset achieves the highest ratings across all dimensions with acceptable inter-annotator agreement (Krippendorff’s α [17] = 0.64–0.78), suggesting that our Generate-then-Verify framework helps mitigate the identified error types. Detailed evaluation protocol is in Appendix E.

4.4 Effectiveness as Training Data

Setup. We fine-tune Qwen2.5-VL-7B-Instruct [34] using LoRA [14] (rank=16, α =32) for one epoch, and evaluate on three scientific figure benchmarks: CharXiv [38] (4,000 descriptive and 1,000 reasoning examples), MMStar [7] (science & technology subset, 250 examples), and MathVista [24] (scientific reasoning subset, 122 examples). For

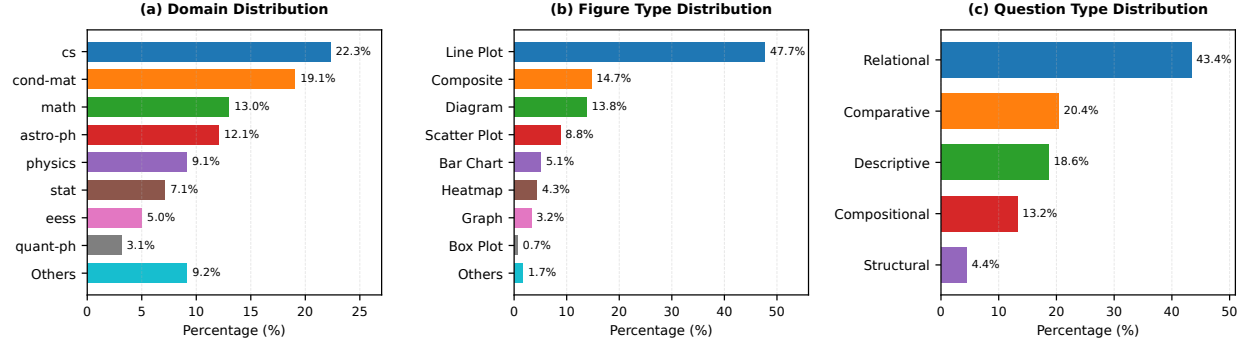


Figure 3: **Dataset Statistics.** Dataset composition across three dimensions: (a) scientific domain distribution across 20 arXiv categories, (b) figure type coverage spanning 12 categories, and (c) question type distribution across five question types. Long-tail categories are grouped as “Others”; complete breakdowns are provided in Appendix C.

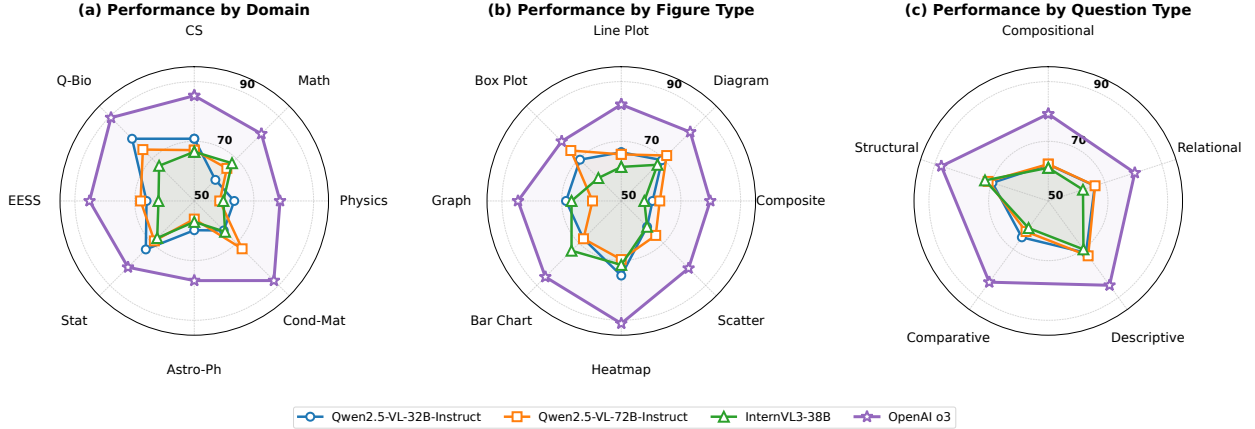


Figure 4: **Dataset Difficulty Assessment.** Model accuracy across (a) scientific domains, (b) figure types, and (c) question types. Even the strongest model (o3) achieves only 77% on Astro-Ph, 80% on Composite figures, and 79% on Compositional questions, revealing substantial challenges. Complete results in Appendix G.

comparison, we train on datasets representing different construction methods: template-based SciFiBench [32] (General.Figure2Caption subset, 500 examples), generation-only ArxivQA [20] (5,000 samples) and SPIQA [31] (figure-type questions only, 5,000 samples), and our dataset (5,000 samples; 500 samples for direct comparison with SciFiBench). Additional training details are in Appendix H.

Results. We report performance gains relative to the original **Qwen2.5-VL-7B-Instruct** model (baseline). As shown in Table 3, training on our dataset yields the best performance across all benchmarks with +2.28% average gain compared to existing scientific figure QA datasets. This demonstrates that QA pairs from our framework effectively transfer to scientific figure understanding capabilities.

Training Data Scaling. To assess the scalability of

Table 3: Baseline performance (absolute %) and gains ($\Delta\%$) for fine-tuned models. CX-D/R: CharXiv Descriptive/Reasoning; MM-ST: MMStar Science & Technology; MV-SR: MathVista Scientific Reasoning.

| Training Data | CX-D | CX-R | MM-ST | MV-SR | Avg. |
|---------------------------|--------------|--------------|--------------|--------------|--------------|
| Baseline (no fine-tuning) | 66.0 | 42.4 | 48.0 | 67.2 | 55.9 |
| SciFiBench (500) | +0.42 | -0.70 | -1.20 | +0.82 | -0.16 |
| ArxivQA (5K) | +0.25 | +0.90 | 0.00 | -1.64 | -0.12 |
| SPIQA (5K) | -0.03 | -0.20 | -1.20 | -1.64 | -0.77 |
| VeriSciQA (500) | +2.00 | -0.40 | +0.80 | 0.00 | +0.60 |
| VeriSciQA (5K) | +2.17 | +1.70 | +3.60 | +1.64 | +2.28 |

Table 4: **Ablation Study.** Performance gains when training on 5K examples from different filtering steps.

| Training Data (5K examples) | Avg. Gain (%) |
|--------------------------------|---------------|
| Generation only (no filtering) | -0.54 |
| With text-based filtering | +0.14 |
| With full verification | +2.28 |

our dataset, we train on varying amounts of data from VERISCIQA (ranging from 500 to 5,000 examples). As shown in Fig. 5, average performance gain scales consistently with training data size, improving nearly 4 \times when increasing from 500 to 5,000 examples (from +0.60% to +2.28%). This consistent scaling trend suggests that our dataset has strong potential for further performance gains with additional training data. Importantly, such scaling is practically feasible: on average, producing one verified QA pair requires approximately 59 open-source API calls (DeepSeek-v3) and 9 closed-source API calls (o4-mini); using publicly available APIs, we achieved a throughput of up to 1,200 verified QA pairs per day.

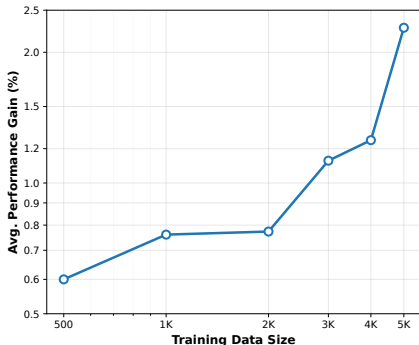


Figure 5: Performance gains when fine-tuning Qwen2.5-VL-7B on increasing amounts of our dataset.

4.5 Ablation Study

Setup. To assess the contribution of each filtering step in our framework, we train on 5,000 QA pairs sampled from different intermediate outputs of the framework (see Table 1): (1) **Generation only:** QA pairs sampled directly after the Generation stage (§3.2), with no filtering applied; (2) **With text-based filtering:** QA pairs sampled after applying text-based filtering (§3.3), before vision-based filtering; (3) **With full verification:** QA pairs sampled after applying both text-based and vision-based filtering. Training and evaluation follow the configuration in §4.4.

Results and Analysis. Training on unfiltered data hurts performance (-0.54%), while text-based filter-

ing provides modest gains (+0.14%). Yet stopping at text-based filtering would yield 2.7 \times more QA pairs (see Table 1). This quantity advantage comes at a severe quality cost: the dataset retains *incorrectly visually grounded* (E1) and *outside-knowledge* (E4) errors that cannot be detected through text-only filtering. Adding vision-based filtering yields a **16 \times performance gain**, confirming that cross-modal verification is essential despite its aggressive filtering rate.

5 Related Work

Scientific Visual Question Answering Datasets. Several SVQA datasets have been proposed to evaluate and train LVLMs on scientific figure understanding. Template-based datasets such as FigureQA [16] and SciFiBench [32] are scalable but limited to fixed question formats. CharXiv [38] offers diverse, high-quality questions through expert annotation, though at the cost of scalability. More recent datasets like ArXivQA [20] and SPIQA [31] leverage LVLMs for generation, achieving larger scale and greater diversity. However, as our audit of ArXivQA reveals (Section 2), generation-only approaches may introduce systematic errors without proper verification. VERISCIQA complements these efforts by providing verified QA pairs through a systematic generation and verification framework, aiming to improve the balance between scale and quality.

Data Synthesis and Verification Techniques. Our methodology builds on recent advances in data synthesis and hallucination mitigation. Similar to self-instruction methods [37], we leverage LLMs to generate data at scale. We face the additional challenge of ensuring quality of generated QA pairs in the cross-modal setting. We propose a *Generate-then-Verify* framework that validates generated QA pairs through cascaded filtering, including cross-modal verification enhanced by self-consistency [36] with majority voting. Unlike general fact-checking methods that rely on external knowledge bases [12, 19, 26], our framework validates QA pairs generated from figure-associated context by checking them against the figures themselves, requiring no external retrieval.

Large Vision-Language Models for Science. The success of recent LVLMs [1, 9, 23, 27] has spurred interest in their application to scientific domains. Benchmarks such as CharXiv [38], SciFiBench [32], and ChartX [13] evaluate LVLMs’ capabilities on scientific figures. These evaluations consistently reveal a significant capability gap: while proprietary models demonstrate strong performance, open-source

counterparts lag behind in scientific visual reasoning. Training datasets for SVQA remain limited in scale or quality. We address this by proposing a framework to construct large-scale, verified data.

6 Conclusion

We introduce a Generate-then-Verify framework for synthesizing reliable SVQA data and instantiate it to build a high-quality dataset VERISCIQA. Our cascaded cross-modal checks substantially reduce common generation errors (E1-E4). Experiments show that current open-source LVLMS struggle on VERISCIQA, while fine-tuning on it improves their performance, with gains that scale with data size, highlighting the promise of continually synthesizing larger SVQA corpora with our framework.

References

- [1] Jean-Baptiste Alayrac, Jeff Donahue, Pauline Luc, Antoine Miech, Iain Barr, Yana Hasson, Karel Lenc, Arthur Mensch, Katherine Millican, Malcolm Reynolds, et al. Flamingo: a visual language model for few-shot learning. *Advances in neural information processing systems*, 35:23716–23736, 2022.
- [2] arXiv. arxiv category taxonomy, 2025. Accessed: 2025-11-13.
- [3] Jinze Bai, Shuai Bai, Shusheng Yang, Shijie Wang, Sinan Tan, Peng Wang, Junyang Lin, Chang Zhou, and Jingren Zhou. Qwen-vl: A versatile vision-language model for understanding, localization, text reading, and beyond, 2023.
- [4] Zechen Bai, Pichao Wang, Tianjun Xiao, Tong He, Zongbo Han, Zheng Zhang, and Mike Zheng Shou. Hallucination of multimodal large language models: A survey. *arXiv preprint arXiv:2404.18930*, 2024.
- [5] Daoyuan Chen, Yilun Huang, Zhijian Ma, Hesen Chen, Xuchen Pan, Ce Ge, Dawei Gao, Yuexiang Xie, Zhaoyang Liu, Jinyang Gao, et al. Data-juicer: A one-stop data processing system for large language models. In *Companion of the 2024 International Conference on Management of Data*, pages 120–134, 2024.
- [6] Daoyuan Chen, Yilun Huang, Xuchen Pan, Nana Jiang, Haibin Wang, Yilei Zhang, Ce Ge, Yushuo Chen, Wenhao Zhang, Zhijian Ma, Jun Huang, Wei Lin, Yaliang Li, Bolin Ding, and Jingren Zhou. Data-juicer 2.0: Cloud-scale adaptive data processing for and with foundation models. In *NeurIPS*, 2025.
- [7] Lin Chen, Jinsong Li, Xiaoyi Dong, Pan Zhang, Yuhang Zang, Zehui Chen, Haodong Duan, Jiaqi Wang, Yu Qiao, Dahua Lin, et al. Are we on the right way for evaluating large vision-language models? *arXiv preprint arXiv:2403.20330*, 2024.
- [8] Zhiyang Chen, Yousong Zhu, Yufei Zhan, Zhaowen Li, Chaoyang Zhao, Jinqiao Wang, and Ming Tang. Mitigating hallucination in visual language models with visual supervision. *arXiv preprint arXiv:2311.16479*, 2023.
- [9] Zhe Chen, Jiannan Wu, Wenhao Wang, Weijie Su, Guo Chen, Sen Xing, Muyan Zhong, Qinglong Zhang, Xizhou Zhu, Lewei Lu, et al. Internvl: Scaling up vision foundation models and aligning for generic visual-linguistic tasks. In *Proceedings of the IEEE/CVF Conference on Computer Vision and Pattern Recognition*, pages 24185–24198, 2024.
- [10] Wenliang Dai, Nayeon Lee, Boxin Wang, Zhuolin Yang, Zihan Liu, Jon Barker, Tuomas Rintamäki, Mohammad Shoeybi, Bryan Catanzaro, and Wei Ping. Nvlm: Open frontier-class multimodal llms. *arXiv preprint arXiv:2409.11402*, 2024.
- [11] Data-Juicer Team. Redpajama-arxiv (refined by data-juicer). <https://huggingface.co/datasets/datajuicer/redpajama-arxiv-refined-by-data-juicer>, 2023. A refined version of ArXiv dataset in RedPajama, containing 1,655,259 samples.
- [12] Luyu Gao, Zhuyun Dai, Panupong Pasupat, Anthony Chen, Arun Tejasvi Chaganty, Yicheng Fan, Vincent Zhao, Ni Lao, Hongrae Lee, Da-Cheng Juan, et al. Rarr: Researching and revising what language models say, using language models. In *Proceedings of the 61st Annual Meeting of the Association for Computational Linguistics (Volume 1: Long Papers)*, pages 16477–16508, 2023.
- [13] Renqiu He, Xiangchao Liu, Rui Zhang, Yichi Han, Chengzhuo Han, Wenjun Zhang, Hang Yu, Zhiyang Zeng, and Shanshan Zhang. Chartx & chartvlm: A versatile benchmark and foundation model for complicated chart reasoning. *arXiv preprint arXiv:2402.12185*, 2024.
- [14] Edward J Hu, Yelong Shen, Phillip Wallis, Zeyuan Allen-Zhu, Yuanzhi Li, Shean Wang, Lu Wang, Weizhu Chen, et al. Lora: Low-rank adaptation of large language models. *ICLR*, 1(2):3, 2022.
- [15] Chaoya Jiang, Haiyang Xu, Mengfan Dong, Jiaying Chen, Wei Ye, Ming Yan, Qinghao Ye, Ji Zhang, Fei Huang, and Shikun Zhang. Hallucination augmented contrastive learning for multimodal large language model. In *Proceedings of the IEEE/CVF Conference on Computer Vision and Pattern Recognition*, pages 27036–27046, 2024.
- [16] Samira Ebrahimi Kahou, Vincent Michalski, Adam Atkinson, Ákos Kádár, Adam Trischler, and Yoshua Bengio. Figureqa: An annotated figure dataset for

- visual reasoning. *arXiv preprint arXiv:1710.07300*, 2017.
- [17] Klaus Krippendorff. *Content analysis: An introduction to its methodology*. Sage publications, 2018.
 - [18] Vladimir I Levenshtein. Binary codes capable of correcting deletions, insertions, and reversals. *Soviet physics doklady*, 10(8):707–710, 1966.
 - [19] Patrick Lewis, Ethan Perez, Aleksandra Piktus, Fabio Petroni, Vladimir Karpukhin, Naman Goyal, Heinrich Küttler, Mike Lewis, Wen-tau Yih, Tim Rocktäschel, et al. Retrieval-augmented generation for knowledge-intensive nlp tasks. *Advances in neural information processing systems*, 33:9459–9474, 2020.
 - [20] Lei Li, Yuqi Wang, Runxin Xu, Peiyi Wang, Xiaochong Feng, Lingpeng Kong, and Qi Liu. Multimodal arxiv: A dataset for improving scientific comprehension of large vision-language models. *arXiv preprint arXiv:2403.00231*, 2024.
 - [21] Yifan Li, Yifan Du, Kun Zhou, Jinpeng Wang, Wayne Xin Zhao, and Ji-Rong Wen. Evaluating object hallucination in large vision-language models. *arXiv preprint arXiv:2305.10355*, 2023.
 - [22] Aixin Liu, Bei Feng, Bing Xue, Bingxuan Wang, Bochao Wu, Chengda Lu, Chenggang Zhao, Chengqi Deng, Chenyu Zhang, Chong Ruan, et al. Deepseek-v3 technical report. *arXiv preprint arXiv:2412.19437*, 2024.
 - [23] Haotian Liu, Chunyuan Li, Qingyang Wu, and Yong Jae Lee. Visual instruction tuning. *Advances in neural information processing systems*, 36:34892–34916, 2023.
 - [24] Pan Lu, Hritik Bansal, Tony Xia, Jiacheng Liu, Chunyuan Li, Hannaneh Hajishirzi, Hao Cheng, Kai-Wei Chang, Michel Galley, and Jianfeng Gao. Mathvista: Evaluating mathematical reasoning of foundation models in visual contexts. *arXiv preprint arXiv:2310.02255*, 2023.
 - [25] Potsawee Manakul, Adian Liusie, and Mark JF Gales. Selfcheckgpt: Zero-resource black-box hallucination detection for generative large language models. *arXiv preprint arXiv:2303.08896*, 2023.
 - [26] Reiichiro Nakano, Jacob Hilton, Suchir Balaji, Jeff Wu, Long Ouyang, Christina Kim, Christopher Hesse, Shantanu Jain, Vineet Kosaraju, William Saunders, et al. Webgpt: Browser-assisted question-answering with human feedback. *arXiv preprint arXiv:2112.09332*, 2021.
 - [27] OpenAI. Gpt-4v(ision) system card. Technical report, OpenAI, 2023.
 - [28] OpenAI. Gpt-4o system card. Technical report, OpenAI, 2024.
 - [29] OpenAI. Introducing o3 and o4-mini, 2025. Accessed: 2025-11-13.
 - [30] OpenAI. Openai o4-mini model card, 2025. Accessed: 2025-10-18.
 - [31] Shraman Pramanick, Rama Chellappa, and Subhashini Venugopalan. Spiqa: A dataset for multimodal question answering on scientific papers. *Advances in Neural Information Processing Systems*, 37:118807–118833, 2024.
 - [32] Jonathan Roberts, Kai Han, Neil Houlsby, and Samuel Albanie. Scifibench: Benchmarking large multimodal models for scientific figure interpretation. *Advances in Neural Information Processing Systems*, 37:18695–18728, 2024.
 - [33] Armin Ronacher. Jinja2: A modern and designer-friendly templating language for python. <https://jinja.palletsprojects.com/>, 2008. Version accessed: 2025.
 - [34] Qwen Team. Qwen2.5-vl, 2025.
 - [35] Peter Tong, Ellis Brown, Penghao Wu, Sanghyun Woo, Adithya Jairam Vedagiri IYER, Sai Charitha Akula, Shusheng Yang, Jihan Yang, Manoj Middepogu, Ziteng Wang, et al. Cambrian-1: A fully open, vision-centric exploration of multimodal llms. *Advances in Neural Information Processing Systems*, 37:87310–87356, 2024.
 - [36] Xuezhi Wang, Jason Wei, Dale Schuurmans, Quoc Le, Ed Chi, Sharan Narang, Aakanksha Chowdhery, and Denny Zhou. Self-consistency improves chain of thought reasoning in language models. *arXiv preprint arXiv:2203.11171*, 2022.
 - [37] Yizhong Wang, Yeganeh Kordi, Swaroop Mishra, Alisa Liu, Noah A Smith, Daniel Khashabi, and Hannaneh Hajishirzi. Self-instruct: Aligning language models with self-generated instructions. In *Proceedings of the 61st annual meeting of the association for computational linguistics (volume 1: long papers)*, pages 13484–13508, 2023.
 - [38] Zirui Wang, Mengzhou Xia, Luxi He, Howard Chen, Yitao Liu, Richard Zhu, Kaiqu Liang, Xindi Wu, Haotian Liu, Sadhika Malladi, et al. Charting gaps in realistic chart understanding in multimodal llms. *Advances in Neural Information Processing Systems*, 37:113569–113697, 2024.
 - [39] Hong Yu, Shashank Agarwal, Mark Johnston, and Aaron Cohen. Are figure legends sufficient? evaluating the contribution of associated text to biomedical figure comprehension. *Journal of biomedical discovery and collaboration*, 4(1):1, 2009.

- [40] Yi-Fan Zhang, Qingsong Wen, Chaoyou Fu, Xue Wang, Zhang Zhang, Liang Wang, and Rong Jin. Beyond llava-hd: Diving into high-resolution large multimodal models. *arXiv preprint arXiv:2406.08487*, 2024.
- [41] Yuze Zhao, Jintao Huang, Jinghan Hu, Xingjun Wang, Yunlin Mao, Daoze Zhang, Zeyinzi Jiang, Zhikai Wu, Baole Ai, Ang Wang, Wenmeng Zhou, and Yingda Chen. Swift:a scalable lightweight infrastructure for fine-tuning, 2024.

Appendix

A Implementation Details

This section provides comprehensive technical details about our Generate-then-Verify framework instantiation to curate VERISCIQA, covering data preparation, generation, and verification stages. A reusable Data-Juicer implementation of the complete framework is detailed in Appendix I.

A.1 Data Preparation

Our framework requires figure-associated context \mathcal{P} (paragraphs that cite the figure) to generate QA pairs via atomic claim extraction (Eq. 2), but existing datasets like ArXivCap [20] provide only figure-caption pairs (F, C) . We therefore augment ArXivCap to construct triplets (F, C, \mathcal{P}) , where \mathcal{P} consists of paragraphs that explicitly cite figure F . We detail this process below.

Data Sources. We use two data sources: ArXivCap³ [20] for figure-caption pairs (F, C) and RedPajama-ArXiv-Refined⁴ [11] for LaTeX source files. Matching by arXiv IDs yields 572K overlapping papers. For each matched paper, we bind its LaTeX source to the figure-caption pairs from ArXivCap. We randomly shuffle this pool and process 44,345 papers in batches to reach our target dataset size.

Context Extraction. For each figure-caption pair (F, C) in a matched paper, we extract its associated context \mathcal{P} from the LaTeX source through the following steps. We first associate figure F with its corresponding `\begin{figure}... \end{figure}` environment by matching captions. Since ArXivCap normalizes captions using `pylatexenc`⁵, we apply the same normalization to LaTeX captions to enable efficient matching via Levenshtein similarity [18] ($\text{sim} \geq 0.9$). We then use regular expressions to extract figure labels from `\label{...}` commands within matched figure environments (including those within subfigure environments). Figures with empty captions, those with ambiguous matches (e.g., duplicate captions in LaTeX source), or those lacking a valid LaTeX label are discarded at this stage. We then identify all paragraphs that cite figure F by searching for the extracted label in `\ref{...}`, `\cref{...}`, and `\autoref{...}` commands using regular expres-

sions. For figures cited in multiple paragraphs, we retain and concatenate all citing paragraphs as context \mathcal{P} .

A.2 Generation

Given triplets (F, C, \mathcal{P}) from data preparation, this stage generates candidate QA pairs through two steps: claim extraction (Eq. 2) and QA pair generation (Eq. 3). We use `deepseek-v3-0324` [22] as M_{text} with temperature $T = 1.0$. All prompts are constructed using Jinja2 [33] templates; complete templates are provided in Appendix B.

Claim Extraction (Eq. 2). We instruct M_{text} to extract atomic claims $\mathcal{S} = \{s_j\}$ from context \mathcal{P} , outputting them within `<Patterns>...</Patterns>` XML tags, with each claim s_j following the pattern “The figure shows...”. If no valid claim can be extracted, the model outputs “None”, and such responses are discarded.

QA Pair Generation (Eq. 3). For each atomic claim $s_j \in \mathcal{S}$, we prompt M_{text} to generate a QA pair $q_j = (Q_j, O_j, A_j^*)$ in XML format. Options O_j contain one correct answer A_j^* (derived from s_j) and three plausible distractors. The model may output “None” if s_j lacks sufficient detail; such cases are discarded.

A.3 Verification

Given candidate QA pairs from generation, this stage applies cascaded filtering (Eq. 1) to retain only high-quality instances. Text-based filtering first ensures source-consistency and visual-dependence without accessing the figure; vision-based filtering then validates each remaining QA candidate against the figure. We use `o4-mini-2025-04-16` [30] as M_{vision} with temperature $T = 1.0$.

Text-Based Filtering. The first step applies two text-only filters without accessing figure F :

Source-Consistency Check (V_{src}). We prompt M_{text} to answer question Q_j from options O_j based solely on source context \mathcal{P} . The model outputs its selected answer in an `<option>` tag, or “None” if the information is insufficient to determine a unique answer. The filter $V_{\text{src}}(Q_j, O_j, A_j^*, \mathcal{P})$ returns **True** only if the model’s selection exactly matches A_j^* , and **False** otherwise (including “None”, multiple answers, or cases where a valid answer cannot be extracted).

Visual-Dependence Check ($V_{\text{vis_dep}}$). To reduce computational cost, we implement this check in two cascaded steps. First, QA pairs are evaluated by `deepseek-v3-0324` given only Q_j , O_j , and caption

³<https://huggingface.co/datasets/MMInstruction/ArxivCap>

⁴<https://huggingface.co/datasets/datajuicer/redpajama-arxiv-refined-by-data-juicer>

⁵<https://github.com/phfaist/pylatexenc>

C ; only candidates where it fails to select A_j^* proceed. Second, remaining candidates are validated by M_{vision} . The filter $V_{\text{vis_dep}}(Q_j, O_j, A_j^*, C)$ returns **True** only if M_{vision} also fails to select A_j^* , indicating that Q_j requires visual information from figure F beyond caption C .

Vision-Based Filtering ($V_{\text{vis_con}}$). We prompt M_{vision} with figure F , caption C , question Q_j , and options O_j to select an answer with reasoning. We perform 3 independent queries and apply 2-of-3 majority voting; candidates with ties are discarded. The filter $V_{\text{vis_con}}(Q_j, O_j, A_j^*, F, C)$ returns **True** only if the majority-voted option matches A_j^* . For retained QA pairs, we store the reasoning from the first query that agrees with the majority answer.

B Complete Prompt Templates

To ensure full reproducibility, this section provides the complete set of prompt templates for all steps of our framework instantiation, including those used for automatic annotation of dataset taxonomies (§4.1). All prompts are implemented using Jinja2 templating syntax.

B.1 Claim Extraction

This prompt implements Eq. 2, instructing M_{text} to extract atomic claims $\mathcal{S} = \{s_j\}$ from figure-associated context \mathcal{P} . Each claim s_j should be self-contained and explicitly describe what figure F shows.

In academic paper writing, authors often use visual charts to support their arguments. Please adopt the perspective of a senior professor in the {{ domain }} field to systematically identify the author’s explanatory discourse about charts from the given paragraph, including but not limited to the following analytical dimensions:

[Analysis Framework]

1. Explicit Reference Localization
 - Direct annotation (e.g., "As shown in Figure 3...")
 - In-paragraph figure number references (e.g., "...results in Fig.2 demonstrate...")
2. Implicit Association Identification
 - Data-driven type (e.g., "The sharp decline indicates..." corresponding to line chart features)
 - Structure mapping type (e.g., "This three-stage process" corresponding to flowchart modules)

3. Multi-dimensional Explanation Perspectives
 - Coordinate analysis (axis labels/unit descriptions)
 - Trend description (linear/non-linear changes)
 - Key point annotation (extreme points/inflection points localization)
 - Comparative argumentation (cross-algorithm/parameter comparison)
 - Method visualization (experimental setup/process diagram)
 - Hypothesis verification (fit between data and theoretical models)

[Processing Requirements]

1. Explicit Reference Localization
 - Must satisfy explicit localization principles:
 - Only extract discourse containing references to charts such as "Figure"/"Fig."
 - Ignore supplementary contextual explanations before and after non-referential parts
2. Pay attention to nested structures:
 - Main and subordinate clauses ("When X exceeds 0.6, as depicted...")
 - Parenthetical supplements ("the throughput (see bar chart)")
3. For the extracted explanatory discourse, please summarize using the sentence pattern "The figure shows...". If multiple points are involved, multiple such sentence patterns can be used to explain separately.
4. Truncation condition: When there is a lack of clear connective words (such as 'therefore', 'however', etc.) between two sentences, even if they appear adjacent in the text, unrelated sentences should not be included in the extracted descriptive content.
5. Please strictly extract only the sentences that contain explicit references to the figure label (e.g., "Fig. X", "Figure X", "Fig.~\ref{fig:...}") and ignore any additional descriptive content that does not directly reference the figure, even if it appears immediately before or after.
6. Extraction must be strictly confined to the sentence that contains the explicit figure label. Any descriptive content outside of this sentence must be excluded, regardless of contextual or semantic relevance.

[Notes]

| | |
|---|--|
| <ul style="list-style-type: none"> - The given paragraph text is in LaTeX format, you only need to focus on the parts referencing images. - Do not infer or add extra information from non-referential sentences, even if they seem contextually related. <p>[Output Specification]</p> <p><Patterns>Please insert your explanatory discourse in a list format using 1. 2. 3., if nothing can be extracted, reply with "None".</Patterns></p> <p>Example 1:</p> <p>Given a paragraph containing "According to the hysteresis loop in Fig.5(b), the remanent magnetization sharply drops when temperature exceeds 300K..." should return:</p> <p><Patterns>1. The figure 5(b) shows that the remanent magnetization sharply drops when temperature exceeds 300K.</Patterns></p> <p>Example 2:</p> <p>Given a paragraph "This study used density functional theory to calculate and analyze the electronic structure of iron-based alloys. After optimizing the lattice parameters, it was found that the density of states distribution near the Fermi surface differs significantly from conventional magnetic materials reported in the literature." should return:</p> <p><Patterns>None</Patterns></p> <p>Please strictly follow this output format.</p> <p>[Task Input]</p> <p>The figure label is</p> <p><figure_label></p> <p>{{ figure_label }}</p> <p></figure_label></p> <p>The figure-citing paragraph is</p> <p><paragraph></p> <p>{{ paragraph }}</p> <p></paragraph></p> | |
|---|--|

B.2 QA Pair Generation

This prompt implements Eq. 3, converting each atomic claim $s_j \in \mathcal{S}$ into a multiple-choice QA pair $q_j = (Q_j, O_j, A_j^*)$ with question Q_j , options O_j , correct answer A_j^* , and plausible distractors.

| | |
|---|--|
| <p>[Background]</p> <p>You are a senior professor in {{ domain }}.</p> <p>Generate rigorous, objective multiple-choice questions (MCQs) for formative assessments</p> | |
|---|--|

to evaluate students' ability to interpret key findings and data from figures in academic papers. These MCQs must be derived exclusively from students' own extracted figure descriptions (e.g., charts, graphs, diagrams) to ensure alignment with their learning materials.

[Requirements]

1. Question Type: Single-choice (2-4 options), with only one correct answer.
2. Focus on Evidence-Based Analysis:
 - Questions must target core conclusions directly supported by visual elements (e.g., trends, comparisons, outliers).
 - Include specific numerical/data points (e.g., "What percentage of users preferred Tool X in Figure 3?") or structural relationships (e.g., "Which layer in the architecture diagram handles encryption?").
3. Distractors: Incorrect options should be academically misleading (e.g., antonyms, approximate values, easily confused terms).
4. Each question must be answered by referring to the figure, do not ask questions like 'According to the description'.
5. When constructing questions, note that you can only receive text input. To ensure the questions can be answered solely by observing the figure, or by reasoning with the figure and the academic paper content, your questions must be based on specific statements referencing the figure, without using content from clauses (unless the clause clearly mentions key elements of the figure, such as colors corresponding to legends or other visual features).
6. If the input description lacks sufficient detail to generate a valid question (e.g., overly vague statements like "Figure 3 shows the experimental results"), immediately return None without explanation.
7. Do not ask about product names, model numbers, protocol versions, or other technical specifications unrelated to visual elements.
8. Explicit Visual References Needed:
 - The description used to generate questions must refer to the figure and include specific data points, labels, or relationships (e.g., "From the figure we know that, DialogueGCN achieves 72% accuracy, while SGED reaches 78%").
 - If the description only mentions general concepts (e.g., "the figure compares two frameworks"), it is insufficient for generating a valid question.
9. Avoid Questions About Elements Not Visually Present:
 - If the figure description does not explicitly

state that an element or data point is depicted in the figure, any question requiring knowledge of that element would fail to meet the requirement for direct visual evidence.

10. Input Description-Centered Questions:

- IMPORTANT: Your questions MUST primarily focus on the content provided in the input description.
- The input description should be the main source for generating questions and determining the correct answers.
- Use the provided section text and caption text only as supplementary context to enhance understanding.
- Do NOT mention the section text or caption text directly in your questions or options.
- Students will NOT see the section text or caption text, so questions must be answerable solely from the figure.
- Incorporate relevant terminology, context, and background naturally, as if this information is common knowledge in the field.
- Only use contextual information that directly relates to elements explicitly mentioned in the input description.

[Output Format]

If you can construct a compliant question, use the following format:

```
<question>Insert your self-contained question
here</question>
<options>
A. Option 1
B. Option 2
C. Option 3
D. Option 4
</options>
<answer>Correct answer (A/B/C/D)</answer>
```

If the input description is insufficient, just output None, without any explanation.

[Example]

```
<question>In the neural network performance
experiment, at which iteration count does
Method A reach its performance inflection
point?</question>
<options>
A. 30% data volume
B. 50% noise intensity
C. 70% iteration count
D. 90% energy threshold
</options>
<answer>C</answer>
```

[Task]

The image label provided: {{ label }}. Only generate questions and options that directly relate to the figure referenced by this label. If the input description mentions multiple image labels, focus exclusively on the figure corresponding to the provided label, and ignore content related to other labels. Do not include the label verbatim in the question or options.

The section text related to the figure is:

```
<section>
{{ section }}
</section>
```

The caption text for the figure is:

```
<caption>
{{ caption }}
</caption>
```

The input description is:

```
<description>
{{ description }}
</description>
```

Generate your self-contained question based primarily on the input description. The question must focus on elements explicitly mentioned in the description. Use the section text and caption text only as supplementary context to enhance understanding, but remember that students will NOT see this contextual information. The question must be answerable by referring to the figure alone.

B.3 Source-Consistency Check

This prompt implements $V_{\text{src}}(Q_j, O_j, A_j^*, \mathcal{P})$, verifying that the correct answer A_j^* can be uniquely determined from the source context \mathcal{P} using M_{text} .

[Background]

You are a senior professor in the field of {{ domain }} with expertise in analyzing academic papers. You are tasked with answering questions about figures from academic papers without directly viewing the images. Instead, you will use the figure label and the text sections that reference the figure to infer what the figure shows and answer questions about it.

[Input]

```
Question: {{ question }}
Options: {{ options }}
Figure Label: {{ figure_label }}
```

Text Referencing Figure: {{ section }}

[Output Format]

<analysis>Insert your analysis here.</analysis>
<option>X</option>

Where X is:

- A single letter (A/B/C/D...) for questions with one correct answer
- Multiple letters separated by commas (e.g., "A,C") for questions with multiple correct answers
- "None" if the information provided is insufficient to determine a unique correct answer

B.4 Visual-Dependence Check

This prompt implements $V_{\text{vis.dep}}(Q_j, O_j, A_j^*, C)$, verifying that question Q_j cannot be answered using only caption C without visual inspection of figure F , using M_{vision} .

[Background]

You are a senior professor in the {{ domain }} field, and now you need to answer a set of multiple-choice questions based on visual question answering (VQA). Although you cannot directly view the images in the questions, you can rely on your deep professional knowledge and logical reasoning abilities, combined with the question descriptions and option content, to provide the most reasonable answers.

[Input]

question: {{ question }}
options: {{ options }}

[Output Format]

Please select the most appropriate answer from the following format:

<option>A/B/C/D...</option>

If the question information is insufficient or a unique correct answer cannot be determined, please output:

<option>None</option>

B.5 Vision-Based Filtering

This prompt implements $V_{\text{vis.con}}(Q_j, O_j, A_j^*, F, C)$, asking M_{vision} to answer question Q_j based solely on figure F and caption C , validating that A_j^* is correctly grounded in the visual content.

[Background]

You are a senior professor in {{ domain }}. Your task is to analyze visual content and answer multiple-choice Visual Question Answering (VQA) questions. Use your expertise to carefully examine the image caption, understand the question context, and select the most accurate answer from the given options.

[Input]

Question: {{ question }}
Options: {{ options }}
Image Caption: {{ caption }}

[Output Format]

<rationale>Insert the reason why you choose the answer.</rationale>

The selected answer:

<option>A/B/C/D...</option>

B.6 Figure Type Annotation

This prompt is used to automatically annotate figure types with GPT-4o for dataset diversity analysis (§4.1).

You are an expert at analyzing scientific figures and charts.

Analyze the given figure and classify it into the most appropriate category.

Respond with ONLY the category name, nothing else.

Classify this figure into ONE of the following categories:

- Line Plot
- Bar Chart
- Pie Chart
- Scatter Plot
- Box Plot
- Heatmap
- Diagram
- Graph
- Photo
- Illustration
- Composite
- Other

Category Definitions and Examples:

1. "Line Plot" - Graphs with continuous lines showing trends, relationships, or functions over time or other continuous variables
Examples: accuracy curves over epochs, loss curves during training, performance comparison lines, ROC curves, function plots

| | |
|--|--|
| <p>, time series trends with confidence intervals (shown as dashed/shaded regions), oscillating signals, distribution curves, multiple overlapping trend lines</p> <p>Key features: connected data points forming continuous lines (smooth or oscillating), x and y axes with continuous quantitative data, legends for multiple lines, may include error bands or confidence intervals, may have multiple panels/subplots but each showing line trends, lines can be smooth curves or high-frequency oscillations</p> <p>NOTE: Even if the figure has multiple subplots/panels, dense oscillations, or many overlapping lines, if each panel primarily shows continuous line trends over a continuous variable (like time), it should ALWAYS be classified as "Line Plot", NOT "Other"</p> | <p>metrics, data point clustering, stem plots (discrete points with vertical lines to axis), parameter sensitivity plots with discrete measurements</p> <p>Key features: individual dots/markers/symbols ('+', 'o', '*', etc.) WITHOUT connecting lines between points, shows relationships between two or more variables, focuses on discrete data points rather than continuous connected lines, may show clear trends but points remain unconnected</p> <p>NOTE: Even if the figure has multiple subplots/panels, if each subplot shows discrete unconnected data points (scatter plots), classify the entire figure as "Scatter Plot", NOT "Other". The key distinguishing feature from "Line Plot" is the ABSENCE of lines connecting the data points</p> |
| <p>2. "Bar Chart" - Graphs using rectangular bars to compare discrete values across categories</p> <p>Examples: method performance comparison (Model A: 85%, Model B: 90%), dataset statistics, accuracy on different benchmarks, ablation study results, grouped bar charts</p> <p>Key features: vertical or horizontal rectangular bars, discrete categories on one axis, quantitative values on the other, often includes error bars or value labels</p> | <p>5. "Box Plot" - Statistical plots showing data distribution through quartiles, used to compare distributions across categories</p> <p>Examples: performance distribution across different methods, statistical comparisons in biological/medical studies, variance analysis across experimental conditions, side-by-side distribution comparisons, violin plots (box plot with density curves)</p> <p>Key features: rectangular boxes representing quartiles (25th, 50th/median, 75th percentiles), whiskers extending to show data range, may include outlier points, often grouped by categories for comparison, primary purpose is showing statistical distribution and variability rather than individual data points</p> <p>NOTE: If you see individual scattered points without box/quartile structure, choose "Scatter Plot" instead. If the focus is on comparing average values rather than distributions, it's likely a "Bar Chart"</p> |
| <p>3. "Pie Chart" - Circular charts divided into slices to show proportions or percentages of categorical data</p> <p>Examples: distribution of error types, proportion of different categories in a dataset, percentage breakdown of survey responses, composition of total (parts of a whole)</p> <p>Key features: circular/pie shape divided into colored slices/wedges, each slice represents a proportion/percentage of categorical data, usually includes percentage labels or category legends showing what each slice represents, slices sum to 100%, primary purpose is to show relative sizes of categories</p> <p>NOTE: NOT for geometric diagrams with radial lines showing angles/directions, or circular schematics with mathematical parameters. If the circle is used to illustrate geometric/physical concepts rather than data proportions, choose "Diagram" instead</p> | <p>6. "Heatmap" - Color-coded grid or matrix showing values through color intensity, including 3D tensor visualizations and scientific intensity maps</p> <p>Examples: confusion matrices, attention weight maps, correlation matrices, similarity matrices, activation maps, 3D tensor/cube visualizations with numerical values in cells, contour plots with color gradients, astronomical intensity maps, microscopy intensity images, scientific observation data visualized as intensity fields</p> <p>Key features: grid structure with cells containing numerical values OR continuous color/grayscale gradients representing data</p> |
| <p>4. "Scatter Plot" - Individual data points plotted to show correlations, distributions, or clusters, including stem plots</p> <p>Examples: t-SNE visualizations, feature space distributions, correlation between two</p> | |

intensity, row and column labels or coordinate axes, may be rendered in 3D but focus is on displaying matrix/tensor/field data, represents measured or computed data values rather than photographic content

7. "Diagram" - Schematic representations, technical diagrams, system architectures, or process flows

Examples: neural network architectures (with boxes/rectangles showing layers), system pipelines, algorithm flowcharts, geometric diagrams with annotations, optical system diagrams, physics/engineering schematics showing mechanical configurations, particle trajectory diagrams, coordinate system illustrations with geometric parameters, circular geometric diagrams with radial lines showing angles/directions/orientations

Key features: uses rectangles/boxes/geometric shapes/curves/circles to represent concepts (not simple circles/dots as graph nodes), focuses on showing processes/workflows/architectures/physical mechanisms/geometric relationships, includes technical annotations and parameters (dimensions, angles, coordinates, mathematical symbols), components are conceptual representations rather than data points, typically shows system configuration or conceptual explanation

NOTE: If the primary focus is graph theory visualization (nodes and edges as mathematical objects), choose "Graph" instead. If the figure shows a grid of cells with numerical values (even in 3D), choose "Heatmap" instead. If you see a circular figure with radial divisions and mathematical parameters (not data percentages), it's likely a geometric diagram, not a pie chart - choose "Diagram"

8. "Graph" - Graph/network visualizations showing nodes and edges as graph-theoretic structures

Examples: graph networks with nodes and edges, social network graphs, knowledge graphs, dependency graphs, tree structures, network topology diagrams, search tree visualizations (A*, BFS/DFS), state transition diagrams

Key features: nodes are typically circles/dots representing graph vertices, edges are lines/arrows representing graph connections, focuses on connectivity and graph structure itself (not process flow), may show different graph configurations or transformations

NOTE: The key distinction is that this

represents graph theory concepts - if you see circles connected by edges showing graph structures, choose this category even if there's some sequential annotation

9. "Photo" - Real photographs captured by cameras, typically used as dataset samples or experimental inputs

Examples: ImageNet sample images, real-world photos for object detection/classification tasks, example images from computer vision datasets, actual photographs used to demonstrate visual phenomena, camera-captured images serving as experimental data

Key features: photographic content from real cameras (not scientific instruments like microscopes or telescopes), natural lighting and realistic textures, shows recognizable real-world objects/scenes/people, should be photographs used as DATA or EXAMPLES without complex methodological annotations

NOTE: If the image shows scientific observation data (astronomical, microscopy, radar, etc.) visualized as intensity maps, choose "Heatmap" instead. If the figure contains photos but is primarily arranged to explain a method/process/comparison with text labels and structured layout (like "before/after", "input/output", "original/perturbed/adversarial"), choose "Diagram" or "Other" instead

10. "Illustration" - Stylized drawings, artistic renderings, synthetic scenes, or conceptual visualizations that are neither data plots nor technical diagrams

Examples: artistic/stylized renderings of biological structures (cell illustrations, organ diagrams), computer-generated scenes (simulated driving environments, game screenshots, robot simulation views), conceptual visualizations (abstract representations of concepts), 3D rendered objects or environments, hand-drawn or digitally illustrated figures that visualize ideas rather than specific data

Key features: non-photographic imagery with artistic or synthetic style, used to illustrate concepts/scenarios/environments rather than present measured data, may be computer-generated (CGI) or hand-drawn, focuses on visual communication of ideas rather than quantitative information

NOTE: If the illustration is primarily a technical schematic with labeled components and annotations, choose "Diagram" instead. If it's a real photograph, choose "Photo"

11. "Composite" - Figures containing multiple

subplots/panels where different subplots belong to DIFFERENT visualization types
 Examples: a figure combining line plots and bar charts together, a panel showing both scatter plots and heatmaps, comparison layouts mixing photos with line plots, figures with one subplot as a diagram and another as a bar chart, multi-panel figures where each panel uses a fundamentally different visualization method (e.g., line plot + confusion matrix + bar chart), methodological figures showing input-output pairs with different visualization types for each stage

Key features: contains multiple distinct subplots/panels/subfigures, each subplot belongs to a different category from the list above (e.g., one is a Line Plot, another is a Bar Chart, another is a Heatmap), the combination is intentional to show different aspects of data/method/results, typically has labels like (a), (b), (c) or organized in a grid layout

NOTE: CRITICAL DISTINCTION - If ALL subplots are of the SAME type (all line plots, all scatter plots, all bar charts, etc.), do NOT use "Composite" - classify it as that specific chart type instead. Only use "Composite" when the subplots genuinely belong to DIFFERENT categories. A figure with 6 line plot panels is "Line Plot", not "Composite". A figure with 3 line plots + 2 bar charts is "Composite"

12. "Other" - Anything that doesn't clearly fit any of the above categories, including unusual or ambiguous visualizations
 Examples: unusual chart types not covered above (radar charts, parallel coordinates, Sankey diagrams, ternary plots), tables with numerical data, text-heavy figures with minimal visualization, ambiguous figures that don't fit standard visualization patterns, figures that are too unclear or low-quality to classify confidently

NOTE: Do NOT use "Other" as a default fallback. Before choosing "Other", carefully verify that the figure is not: (1) a standard chart type with multiple panels of the SAME type, or (2) a composite figure with multiple panels of DIFFERENT types. "Other" should only be used for truly unusual or ambiguous cases that don't fit any of the 11 categories above

Instructions:

- Carefully examine the figure's visual characteristics and PRIMARY PURPOSE
- Choose the SINGLE most appropriate category

based on what the figure is trying to COMMUNICATE, not just what it contains

- For scientific papers: data visualization plots (Line/Bar/Pie/Scatter/Box/Heatmap) should be distinguished from structural diagrams (Diagram/Graph) and image content (Photo/Illustration)
- ****CRITICAL for multi-panel figures****:
 - * If ALL subplots are the SAME chart type (e.g., all line plots, all scatter plots, all bar charts), classify as THAT specific chart type, NOT "Composite" or "Other"
 - * If subplots belong to DIFFERENT types (e.g., line plot + bar chart, scatter + heatmap), classify as "Composite"
 - * Only use "Other" for truly unusual visualizations that don't fit any of the 11 defined categories
- If a figure contains photos but is arranged to explain a method/process/comparison (with text like "Input", "Output", "Before", "After"), consider "Diagram" or "Composite" depending on whether other visualization types are mixed in
- When in doubt, consider: Is this showing QUANTITATIVE DATA (Line/Bar/Pie/Scatter/Box/Heatmap), STRUCTURAL RELATIONSHIPS (Diagram/Graph), VISUAL EXAMPLES (Photo/Illustration), MIXED VISUALIZATIONS (Composite), or UNUSUAL TYPES (Other)?

Respond with ONLY the exact category name from the list above (e.g., "Bar Chart", "Box Plot", "Graph", "Photo", "Illustration", "Composite").

B.7 Question Type Annotation

This prompt is used to automatically annotate question types with GPT-4o for dataset diversity analysis (§4.1).

You are an expert at analyzing scientific question-answering tasks and cognitive reasoning patterns.
 Your task is to classify questions based on their cognitive requirements.
 You must respond with ONLY a valid JSON object, nothing else.
 Analyze the following scientific figure question and classify it based on cognitive operations required.

```
**Question**: {{ question }}
**Answer**: {{ answer }}
**Options**: {{ options }}
```

| | |
|--|--|
| <p>---</p> <p>**Cognitive Type Definitions:**</p> <ol style="list-style-type: none"> 1. **Descriptive** - Reading or identifying a single value, label, or attribute from the figure <ul style="list-style-type: none"> - Examples: "What is the accuracy of Model A?", "Which color represents the baseline?", "What is the value at epoch 10?" - Key feature: Direct value extraction or identification, no comparison or computation 2. **Comparative** - Comparing two or more entities based on quantitative or qualitative measures (magnitude, quality, ranking) <ul style="list-style-type: none"> - Examples: "Which model performs best?", "Is Model A better than Model B?", "Which dataset shows the highest accuracy?", "Which method is faster?" - Key feature: Comparing MAGNITUDE, QUALITY, or RANKING (better/worse/larger/smaller/higher/lower/best/worst/fastest/slowest) 3. **Relational** - Identifying trends, patterns, correlations, states, or relationships between variables <ul style="list-style-type: none"> - Examples: "Does the loss curve show convergence?", "What is the relationship between learning rate and accuracy?", "Is there a positive correlation?", "Which curve corresponds to the fluid state?" - Key feature: Analyzing patterns, trends, relationships, or matching states/characteristics rather than comparing magnitudes 4. **Compositional** - Aggregation, computation, or multi-step reasoning involving multiple values <ul style="list-style-type: none"> - Examples: "What is the average of values A, B, and C?", "What is the sum of all baseline scores?", "What is the difference between A and B?", "How many models are shown in the legend?" - Key feature: Requires calculation, aggregation, counting, or combining multiple pieces of information 5. **Structural** - Understanding figure organization, architecture, flow, or structural relationships <ul style="list-style-type: none"> - Examples: "What component follows the attention layer?", "How many stages are in the pipeline?", "What is the overall architecture?" - Key feature: Understanding structural organization or architectural design | <p>---</p> <p>**Task:**</p> <p>Identify the **Primary Type**: The MAIN cognitive goal of the question (choose exactly ONE from the 5 types above)</p> <p>**Examples:**</p> <p>Example 1: Question: "What is the accuracy of Model A?" Answer: "92.3%" Response: {"primary_type": "Descriptive"}</p> <p>Example 2: Question: "Which model achieves higher accuracy, Model A or Model B?" Answer: "Model A" Response: {"primary_type": "Comparative"}</p> <p>Example 3: Question: "What is the average improvement of Model A over baseline across all epochs?" Answer: "5.2%" Response: {"primary_type": "Compositional"}</p> <p>Example 4: Question: "Does the loss curve show convergence?" Answer: "Yes" Response: {"primary_type": "Relational"}</p> <p>Example 5: Question: "What component follows the attention mechanism in the architecture?" Answer: "Feed-Forward Network" Response: {"primary_type": "Structural"}</p> <p>---</p> <p>**Instructions:**</p> <ol style="list-style-type: none"> 1. Read the question carefully and examine the figure image 2. Identify what cognitive operation is needed to answer the question: <ul style="list-style-type: none"> - **Descriptive**: Directly read or identify a single value/label - **Comparative**: Compare multiple entities based on magnitude, quality, or ranking - **Relational**: Analyze patterns, trends, relationships, or identify states - **Compositional**: Count, calculate, aggregate, or combine multiple values - **Structural**: Understand organization, flow, or architectural relationships 3. Respond with ONLY a JSON object in this exact |
|--|--|

```
format:
{"primary_type": "<one of the 5 types>"}
Now classify the question above:
```

C Dataset Taxonomies

This section provides detailed definitions and complete distribution tables for the three key dimensions of VERISCIQA: figure types, question types, and scientific domains. Scientific domain labels are assigned according to the arXiv category taxonomy of the source papers, while figure types and question types are automatically annotated using GPT-4o with carefully designed prompts (see Appendix B.6 and B.7).

C.1 Figure Type Taxonomy

We categorize figures in our dataset into 12 distinct types based on their visual structure and information encoding. This diversity helps models generalize across different visualization modalities and enables fine-grained performance analysis.

Figure Type Definitions. Our figure taxonomy encompasses both data visualization charts and structural representations:

- **Line Plot** (47.7%): Graphs with continuous lines showing trends, relationships, or functions over continuous variables. Examples include accuracy curves over epochs, loss curves during training, and time series with confidence intervals.
- **Composite** (14.7%): Figures containing multiple subplots/panels where different subplots belong to different visualization types (e.g., combining line plots with bar charts, or mixing scatter plots with heatmaps). Note: Figures with multiple subplots of the same type are classified into that specific type, not as Composite.
- **Diagram** (13.8%): Schematic representations including neural network architectures, system pipelines, algorithm flowcharts, geometric diagrams, and physics/engineering schematics with technical annotations.
- **Scatter Plot** (8.8%): Individual data points plotted without connecting lines, showing correlations, distributions, or clusters. Examples include t-SNE visualizations and feature space distributions.
- **Bar Chart** (5.1%): Rectangular bars comparing discrete values across categories, commonly used

for method performance comparison and ablation study results.

- **Heatmap** (4.3%): Color-coded grids or matrices showing values through color intensity, including confusion matrices, attention maps, and correlation matrices.
- **Graph** (3.2%): Graph/network visualizations showing nodes and edges as graph-theoretic structures, including knowledge graphs and dependency graphs.
- **Box Plot** (0.7%): Statistical plots showing data distribution through quartiles, used to compare distributions across categories.
- **Other** (0.5%): Unusual chart types not covered by standard categories, such as radar charts, parallel coordinates, and Sankey diagrams.
- **Illustration** (0.5%): Stylized drawings or artistic renderings, including computer-generated scenes and conceptual visualizations.
- **Photo** (0.5%): Real photographs captured by cameras, typically used as dataset samples or experimental inputs.
- **Pie Chart** (0.2%): Circular charts divided into slices showing proportions or percentages of categorical data.

The complete distribution is shown in Table 5. Line plots dominate the dataset (47.7%), reflecting their prevalence in scientific publications for showing experimental results and trends. Composite figures (14.7%) and diagrams (13.8%) are also common, highlighting the complexity of scientific communication that often requires multiple visualization modalities or structural explanations.

C.2 Question Type Taxonomy

We define 5 question types based on the cognitive operations required to answer them. This diversity helps models generalize across different reasoning operations and enables fine-grained performance analysis.

Question Type Definitions. Our cognitive taxonomy categorizes questions by the primary reasoning operation required:

- **Relational** (43.4%): Identifying trends, patterns, correlations, states, or relationships between variables. Examples: “Does the loss curve show convergence?”; “What is the relationship between learning rate and accuracy?”; “Which curve corresponds to the fluid state?”

| Figure Type | Count | Percentage |
|--------------|---------------|---------------|
| Line Plot | 9,710 | 47.7% |
| Composite | 2,983 | 14.7% |
| Diagram | 2,808 | 13.8% |
| Scatter Plot | 1,790 | 8.8% |
| Bar Chart | 1,035 | 5.1% |
| Heatmap | 880 | 4.3% |
| Graph | 659 | 3.2% |
| Box Plot | 141 | 0.7% |
| Other | 111 | 0.5% |
| Illustration | 98 | 0.5% |
| Photo | 95 | 0.5% |
| Pie Chart | 41 | 0.2% |
| Total | 20,351 | 100.0% |

Table 5: Distribution of figure types in our dataset. The taxonomy covers 12 distinct visualization modalities, from standard data plots (Line Plot, Bar Chart) to structural representations (Diagram, Graph) and composite multi-panel figures.

- **Comparative** (20.4%): Comparing two or more entities based on quantitative or qualitative measures (magnitude, quality, ranking). Examples: “Which model performs best?”; “Is Model A better than Model B?”; “Which dataset shows the highest accuracy?”
- **Descriptive** (18.6%): Reading or identifying a single value, label, or attribute directly from the figure. Examples: “What is the accuracy of Model A?”; “Which color represents the baseline?”; “What is the value at epoch 10?”
- **Compositional** (13.2%): Aggregation, computation, or multi-step reasoning involving multiple values. Examples: “What is the average of values A, B, and C?”; “What is the sum of all baseline scores?”; “How many models are shown in the legend?”
- **Structural** (4.4%): Understanding figure organization, architecture, flow, or structural relationships. Examples: “What component follows the attention layer?”; “How many stages are in the pipeline?”; “What is the overall architecture?”

The complete distribution is shown in Table 6. Relational questions dominate (43.4%), indicating that scientific figure understanding heavily relies on pattern recognition and relationship analysis rather than simple value extraction. This distribution reflects the analytical nature of scientific inquiry, where understanding trends and correlations is more valuable than reading individual data points.

| Question Type | Count | Percentage |
|---------------|---------------|---------------|
| Relational | 8,825 | 43.4% |
| Comparative | 4,145 | 20.4% |
| Descriptive | 3,795 | 18.6% |
| Compositional | 2,686 | 13.2% |
| Structural | 900 | 4.4% |
| Total | 20,351 | 100.0% |

Table 6: Distribution of question types in our dataset based on cognitive operations. The taxonomy emphasizes higher-order reasoning skills (Relational, Comparative, Compositional) over simple value extraction (Descriptive).

C.3 Scientific Domain Taxonomy

Our dataset spans 20 arXiv primary categories, covering diverse scientific fields from computer science and physics to biology and economics. This broad coverage helps models generalize across scientific domains with varying visual conventions and terminology, and enables fine-grained performance analysis.

Domain Coverage. The distribution across scientific domains is shown in Table 7. Computer Science (cs, 22.3%) and Condensed Matter Physics (cond-mat, 19.1%) are the most represented categories, followed by Mathematics (math, 13.0%) and Astrophysics (astro-ph, 12.1%). This distribution reflects both the prevalence of these fields on arXiv and their heavy reliance on visual figures for communicating results. The dataset also includes substantial representation from applied sciences (Statistics, Electrical Engineering, Quantitative Biology) and physical sciences (high-energy physics, nuclear physics, quantum physics), ensuring broad domain coverage.

D Filtering Analysis

In §4, we demonstrated that our Generate-then-Verify framework produces higher-quality QA pairs compared to existing datasets through both human evaluation (§4.3) and effectiveness as training data (§4.4). To validate the effectiveness of each step, we conduct small-scale human evaluation on rejected instances. Results suggest the framework effectively identifies and removes the error types (E1–E4) identified in §2.

D.1 QA Pair Generation Analysis

During the QA pair generation step, M_{text} was instructed to decline producing QA pairs from atomic claims that are too vague or lack sufficient grounding

| ArXiv Category | Count | % |
|---|---------------|--------------|
| cs (Computer Science) | 4,541 | 22.3 |
| cond-mat (Condensed Matter) | 3,878 | 19.1 |
| math (Mathematics) | 2,648 | 13.0 |
| astro-ph (Astrophysics) | 2,456 | 12.1 |
| physics (Physics) | 1,854 | 9.1 |
| stat (Statistics) | 1,451 | 7.1 |
| eess (Electrical Engineering and Systems Science) | 1,019 | 5.0 |
| quant-ph (Quantum Physics) | 640 | 3.1 |
| nlin (Nonlinear Sciences) | 577 | 2.8 |
| q-bio (Quantitative Biology) | 527 | 2.6 |
| hep-ph (High Energy Physics – Phenomenology) | 219 | 1.1 |
| nucl-th (Nuclear Theory) | 124 | 0.6 |
| gr-qc (General Relativity and Quantum Cosmology) | 104 | 0.5 |
| hep-th (High Energy Physics – Theory) | 75 | 0.4 |
| q-fin (Quantitative Finance) | 69 | 0.3 |
| nucl-ex (Nuclear Experiment) | 49 | 0.2 |
| math-ph (Mathematical Physics) | 45 | 0.2 |
| hep-lat (High Energy Physics – Lattice) | 26 | 0.1 |
| hep-ex (High Energy Physics – Experiment) | 26 | 0.1 |
| econ (Economics) | 23 | 0.1 |
| Total | 20,351 | 100.0 |

Table 7: Distribution of scientific domains (arXiv primary categories) in our dataset. The broad coverage across 20 categories ensures domain diversity and generalization capability.

(as described in §3.2). To evaluate whether this rejection mechanism works as expected, we randomly sampled 30 rejected claims from the dataset curation process and manually evaluated them.

Evaluation Results. Among the 30 sampled rejected claims:

- **Good (7 claims, 23.3%):** These atomic claims were actually suitable for QA generation but rejected due to M_{text} limitations. However, given the large pool of atomic claims available, this does not hinder the scalability of the framework.
- **Too Vague (23 claims, 76.7%):** These atomic claims lacked sufficient grounding to generate valid QA pairs. They either lacked specific visual elements (e.g., data points, labels, structural relationships), or used subjective qualitative descriptors without quantitative grounding (e.g., “good results”, “nearly indistinguishable”), making it difficult to construct objective, verifiable questions. See qualitative examples in Appendix F.

Discussion. The analysis reveals that the generation refusal mechanism effectively filters unsuitable claims, with approximately 76.7% of rejections being justified. While 23.3% of rejections are due to

M_{text} limitations, the large pool of atomic claims ensures this does not impact the framework’s ability to scale. The “too vague” cases can be attributed to authors’ writing style in scientific papers, where figure descriptions are often briefly mentioned or glossed over in the main text without providing sufficient detail. When authors reference figures, they frequently use high-level or qualitative descriptions, assuming readers will examine the figure directly for specifics.

D.2 Text-Based Filtering Analysis

As described in §3.3, text-based filtering applies two checks: source-consistency and visual-dependence. To verify these filters work as intended, we randomly sampled 50 QA pairs rejected after each step and manually evaluated them.

Evaluation Results. For the 50 sampled instances rejected by the source-consistency check:

- **Valid rejection (36 instances, 72.0%):** M_{text} was unable to uniquely identify one correct answer from the provided options based on the source context, indicating genuine inconsistencies or ambiguities in the generated QA pairs.
- **Over-filtering (14 instances, 28.0%):** Valid QA pairs that were rejected due to M_{text} limitations or overly aggressive prompting, but should have been retained.

For the 50 sampled instances rejected by the visual-dependence check:

- **Valid rejection (33 instances, 66.0%):** Questions that can be answered or reasonably inferred without viewing the figure, either from the caption alone or from general knowledge, correctly identifying non-visual questions (E3). Notably, some questions can be answered by reasoning through the answer options, which suggests that constructing more challenging distractor options could further improve question difficulty and visual dependence.
- **Over-filtering (17 instances, 34.0%):** Valid visual questions that were incorrectly rejected. When we instruct M_{text} to attempt answering the question given only the caption, M_{text} sometimes makes lucky guesses on questions that genuinely require visual information, accidentally matching the correct answer A^* . This causes the filter to mistakenly classify these visual-dependent questions as answerable without the figure, leading to false rejections.

Discussion. The text-based filtering achieves 72.0% and 66.0% precision for source-consistency and visual-dependence checks respectively. The over-filtering rates (28.0% and 34.0%) reflect trade-offs in the filtering design: for source-consistency, aggressive prompting helps catch genuine inconsistencies but may be overly strict; for visual-dependence, M_{vision} sometimes makes lucky guesses on genuinely visual questions. These results suggest that the text-based filtering works as intended.

D.3 Vision-Based Filtering Analysis

As described in §3.3, vision-based filtering validates that the answer is visually grounded in the figure and does not require outside knowledge, primarily targeting *incorrectly visually grounded* (E1) and *outside-knowledge* (E4) errors. To verify this filter works as intended, we randomly sampled 50 QA pairs rejected at the vision-based filtering and manually evaluated them.

Evaluation Results. The breakdown of the 50 sampled rejected instances is as follows:

- **Incorrectly visually grounded (E1) (25 instances, 50.0%):** The generated questions reference visual elements that are not present or not correctly represented in the figure. In most cases, M_{text} hallucinates details when generating questions from atomic claims. In the remaining cases, the atomic claim itself contains information that does not correspond to the visual content, representing author errors. See Figure 21 in Appendix F for an example.
- **Outside-knowledge required (E4) (16 instances, 32.0%):** The questions require information not visually available in the figure or caption. This error stems from M_{text} generating QA pairs conditioned on figure-associated context \mathcal{P} , which may include information not present in the figure (e.g., precise numerical values, experimental settings, or quantitative details only mentioned in surrounding text). See Figure 22 in Appendix F for an example.
- **Over-filtering due to model limitations (9 instances, 18.0%):** Valid QA pairs where the answer is visually grounded and answerable from the figure, but models failed to provide the correct response due to its inherent capability limitations.

Discussion. The vision-based filtering demonstrates strong precision (82.0%) in identifying genuinely problematic QA pairs, successfully catching E1 and

E4 errors that slipped through text-based filtering. The relatively low over-filtering rate (18.0%) suggests that aggressive vision-based filtering is justified, as it removes 82% problematic cases while only sacrificing 18% valid instances due to M_{vision} limitations. Combined with the ablation study results (§4.5) showing 16 \times performance gains from vision-based filtering, these findings suggest that ensuring visual grounding correctness and self-containment (not requiring outside knowledge) plays a critical role in dataset quality.

E Human Evaluation Protocol

We describe the interface and annotation guidelines used in our human evaluation study (§ 4.3). We recruited 10 annotators who are CS graduate students. To ensure annotation quality, annotators were asked to read detailed guidelines before the annotation session. For each evaluation dimension, we provided concrete examples with ratings at each score level (1, 3, 5) to calibrate their understanding of the rating scale.

E.1 Annotation Interface

We developed a web-based annotation interface that presents annotators with a figure F , caption C , question Q , answer options O , and the designated correct answer A^* (following the notation from § 3.1). For QA pairs without captions (e.g., samples from baseline datasets like ArxivQA), the caption field is not displayed. Annotators were not provided with any background information about the datasets or our project to ensure unbiased evaluation. They evaluate each QA pair along multiple dimensions based solely on the presented information. Figure 6 shows a screenshot of the interface.

E.2 Annotation Guidelines

We conducted human evaluation to assess the quality of our dataset across five key dimensions. This subsection presents the detailed annotation guidelines provided to human annotators.

Overview. For each VQA sample, annotators were shown the figure F , caption C , question Q , answer options O , correct answer A^* , and rationale. They were asked to rate the sample on five dimensions using a 5-point Likert scale (1 = lowest quality, 5 = highest quality). For each dimension, we provide anchor descriptions at scores 1, 3, and 5; annotators may assign intermediate scores (2 or 4) for cases falling between these anchors.

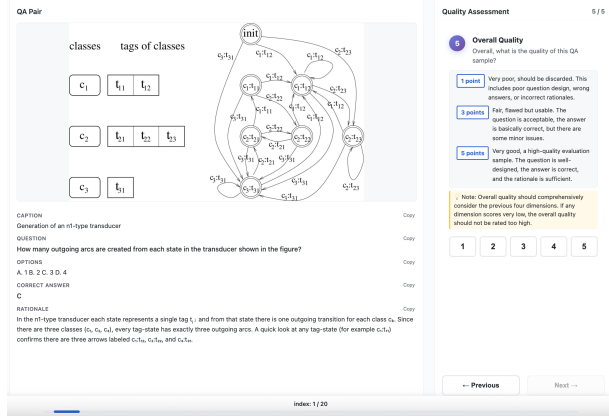


Figure 6: Screenshot of the web-based annotation interface. The left panel displays the question information (figure, caption, question, options, correct answer, and rationale), while the right panel presents a carousel of rating cards for the five evaluation dimensions. Annotators rate each dimension on a 5-point Likert scale before submitting their assessment.

Dimension 1: Factual Correctness

Definition. To what extent is the question, answer, and rationale explicitly supported by the visual information in the figure?

Rating Criteria:

- **1 point:** Completely incorrect or contradicts the figure. This includes wrong answers, completely incorrect rationales, or hallucinated question content (asking about elements not present in the figure).
- **3 points:** Ambiguous or partially correct. The answer may be correct but the rationale is insufficient, or the answer might be correct but the evidence is unclear.
- **5 points:** Completely correct. The question is based on actual figure content, the answer is accurate, and the rationale has clear visual evidence support.

Note: Question hallucination (asking about content not present in the figure) counts as factually incorrect and should be rated 1 point.

Dimension 2: Intent Alignment

Definition. To what extent does the question reflect the core scientific information that the figure is intended to convey?

Rating Criteria:

- **1 point:** Completely irrelevant, such as treating a schematic diagram as a landscape photo. The question completely misses the scientific intent.

- **3 points:** Somewhat off-target but still within a reasonable range. The question asks about secondary information in the figure rather than its main message.
- **5 points:** Highly aligned with the scientific intent of the figure. The question asks about the core information the figure is meant to communicate.

Note: Even if the answer is correct, if the question focuses on marginal information rather than core content of the figure, it should not receive a high score.

Dimension 3: Visual Dependency

Definition. If you only see the question and options without viewing the figure, how difficult would it be to answer this question?

Rating Criteria:

- **1 point:** Very easy. The answer is common sense or already given in the question text, indicating the question does not require viewing the figure.
- **3 points:** Possibly guessable but uncertain. The question design is mediocre in requiring visual information.
- **5 points:** Absolutely impossible to answer without the figure. The question has strong dependency on visual information.

Note: High-quality VQA questions should require models to examine the figure to answer, rather than relying on guessing or background knowledge alone.

Dimension 4: Self-Containment

Definition. Does answering this question require knowledge beyond the figure, caption, and question text that is specific to this particular paper (e.g., special symbol definitions, specific experimental settings mentioned elsewhere in the paper)?

Rating Criteria:

- **1 point:** Absolutely requires paper-specific knowledge (such as symbol definitions or experimental settings defined elsewhere in the paper) to answer. The question cannot be answered without reading the full paper (unless this information is provided in the caption).
- **3 points:** Requires some paper-specific background, but can be reasonably inferred from the figure, caption, and general domain knowledge.
- **5 points:** Completely self-contained. All necessary information is provided in the figure, caption, or question text.

Note: Basic academic common sense and general domain knowledge (such as “accuracy”, “temperature”,

and other standard concepts) are acceptable and do not count as “external knowledge”. This dimension only evaluates whether paper-specific information beyond what is shown is required.

Dimension 5: Overall Quality

Definition. Overall, what is the quality of this QA sample?

Rating Criteria:

- **1 point:** Very poor, should be discarded. This includes poor question design, wrong answers, or incorrect rationales.
- **3 points:** Fair, flawed but usable. The question is acceptable, the answer is basically correct, but there are some minor issues.
- **5 points:** Very good, a high-quality evaluation sample. The question is well-designed, the answer is correct, and the rationale is sufficient.

Note: Overall quality should comprehensively consider the previous four dimensions. If any dimension scores very low, the overall quality should not be rated too high.

F Additional Qualitative Examples

We provide additional examples to illustrate: (1) QA pairs constructed by our framework and included in VERISCIQA, and (2) error cases captured and filtered out at each step.

F.1 QA Pairs in VeriSciQA

We present representative examples that demonstrate the diversity and quality of VERISCIQA across different figure types and question complexities.

Example 1

Figure: 7

Caption: From left to right, the conceptual structures of CALPA-XuNet2, XuNet2, SRNet, and CALPA-SRNet* are illustrated respectively. The number and corresponding shrinking rate of output channels of every convolutional layer is shown alongside the representing bar. For SRNet and CALPA-SRNet, blue “L1” to “L12” represent twelve composition blocks following the notations in cite.

Question: In the SRNet structure shown in the figure, which blocks use transformed shortcut connections?

Options:

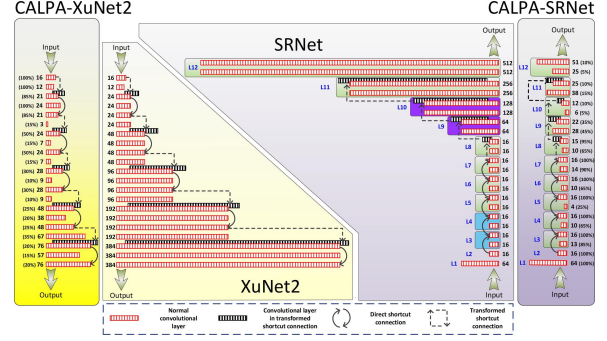


Figure 7: Figure for QA Pair in VERISCIQA

- A. L1 and L2
- B. L3 and L4
- C. L9 and L10
- D. L11 and L12

Answer: C

Reasoning: In the SRNet sketch only the residual blocks where the channel-width steps up require a 1×1 convolution in the shortcut (shown as a dashed “transformed” arrow and a striped conv block). These occur at L9 ($16 \rightarrow 64$ channels) and L10 ($64 \rightarrow 128$ channels). The earlier blocks all use direct (identity) shortcuts, and L11/L12 have no transformed shortcut in SRNet. Hence the transformed shortcuts appear only at L9 and L10.

Example 2

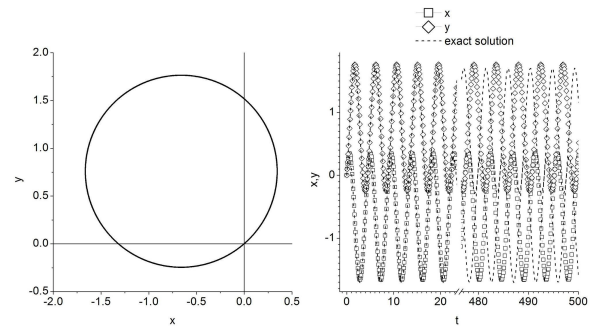


Figure 8: Figure for QA Pair in VERISCIQA

Figure: 8

Caption: Simulated evolution of the particle using our numerical integrator constructed from a DSOCs for $k = 1$, $x(t) = y(t) = 0$ and $\dot{x}(0) = \dot{y}(0) = 1$. Constant time step used: $h = 0.1$. LEFT: trajectory on the plane, RIGHT: comparison between our approximation and the exact solutions of x and y over two time intervals

Question: At what time does the maximum difference between the simulated evolution and the exact

solution occur in the figure?

Options:

- A. Near $t=100$
- B. Near $t=300$
- C. Near $t=500$
- D. Near $t=700$

Answer: C

Reasoning: In the comparison plot on the right, the numerical markers (squares and diamonds) almost exactly follow the dashed exact curves at early times, but by the end of the simulation (around $t=500$) the dashed and marker curves are visibly out of phase, showing the largest accumulated error. No data is shown near $t=700$, so the maximum difference clearly occurs near $t=500$.

Example 3

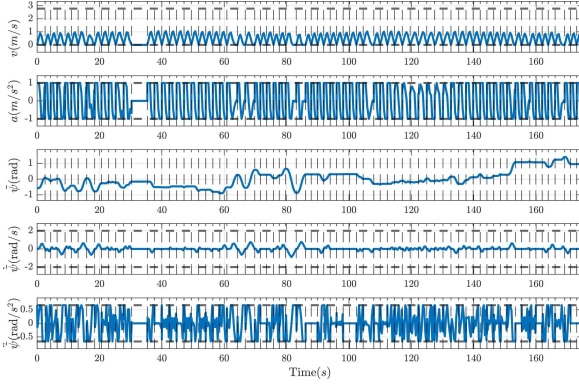


Figure 9: Figure for QA Pair in VERISCIQA

Figure: 9

Caption: Motion trajectory generated by iteratively solving OCP of each segment.

Question: What is the approximate total time taken to complete the motion trajectory shown in the figure?

Options:

- A. ≈ 90 seconds
- B. ≈ 180 seconds
- C. ≈ 270 seconds
- D. ≈ 360 seconds

Answer: B

Reasoning: The horizontal axis of the trajectory plots spans from 0 up to just under 180 s (with the final tick at 160 s and the trace ending around 170 s), so the total maneuver duration is on the order of 180 seconds.

Example 4

Figure: 10

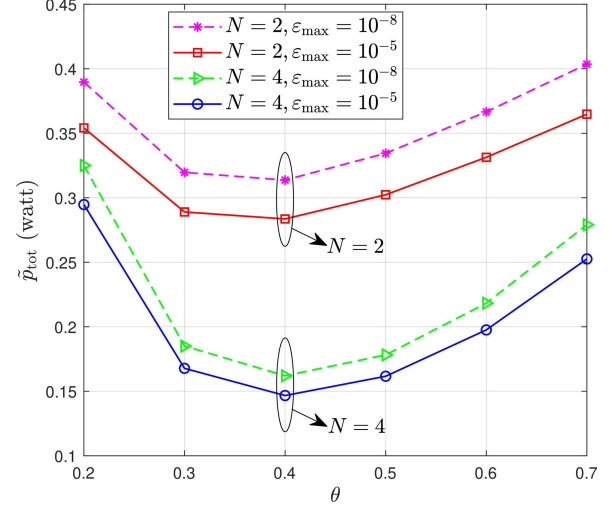


Figure 10: Figure for QA Pair in VERISCIQA

Caption: \tilde{P}_{tot} versus θ under different values of N and ϵ_{max} for $\theta = 0.5$, $K = 5$, $B = 1000$ bits.

Question: At which values of θ does the figure show that the required power consumption is high?

Options:

- A. $\theta = 0.1$ and $\theta = 0.3$
- B. $\theta = 0.2$ and $\theta = 0.7$
- C. $\theta = 0.4$ and $\theta = 0.6$
- D. $\theta = 0.5$ and $\theta = 0.8$

Answer: B

Reasoning: The plot of total power \tilde{P}_{tot} versus θ shows a U-shaped curve for all curves: power is high at the two ends of the θ range (around $\theta = 0.2$) and rises again at the upper end ($\theta = 0.7$), with its minimum near $\theta = 0.4$. Hence, the required power is highest at $\theta = 0.2$ and $\theta = 0.7$.

Example 5

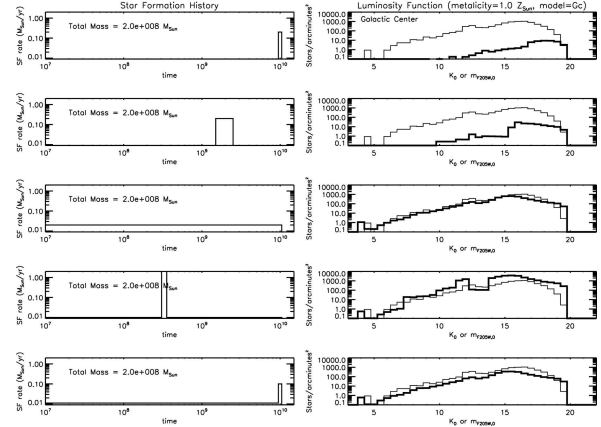


Figure 11: Figure for QA Pair in VERISCIQA

Figure: 11

Caption: A figure adapted from `jcit.j` showing various star formation scenarios (left), and resultant model luminosity functions (right, thick) compared to observed luminosity functions (right, thin) in the GC. The models assume a Salpeter IMF slope, an elevated lower-mass turnover of 10, and are additionally constrained to produce 2×10^8 in stars within the region. The observations have been corrected for incompleteness. The third panels from the top, i.e. continuous star formation, best fit the data. The observed turn-down at the faint end appears to be real and is only well fit only by assuming a very high lower mass turnover.

Question: At what dereddened K-band magnitude does the observed luminosity function of the field in the GC show a turn-down?

Options:

- A. Greater than 12
- B. Greater than 14
- C. Greater than 16
- D. Greater than 18

Answer: C

Reasoning: In the luminosity-function panels, the observed (thin) counts rise up to $K_0 \approx 15$ and then begin to fall off at fainter magnitudes. The drop-off (“turn-down”) occurs just beyond $K_0 \approx 16$, matching the continuous-star-formation model only if one imposes a high low-mass cutoff. Thus the observed LF turns down at dereddened K-band magnitudes greater than 16.

Example 6

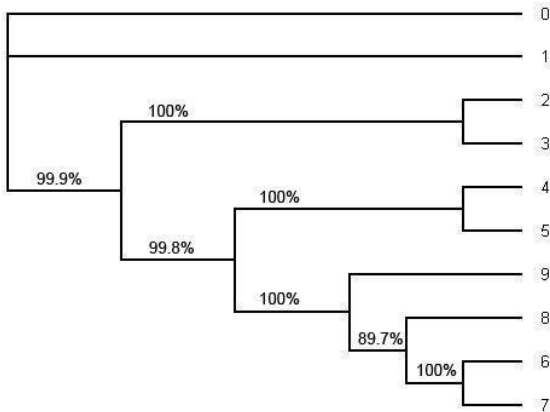


Figure 12: Figure for QA Pair in VERISCIQA

Figure: 12

Caption: The ML tree estimated by the software PHYML under HKY model from the whole align-

ment (including position 1 through position 1505). This is an unrooted tree. The number in each split represents the probability of the split estimated by bootstrapping with the bootstrap sample size 1000. Note that the tree topology of the ML tree is the same as the tree topology of the consensus tree in Fig. and the tree topology in Fig.

Question: What is the approximate support value for the split with the lowest probability in the ML tree under the HKY model?

Options:

- A. 50%
- B. 70%
- C. 90%
- D. 100%

Answer: C

Reasoning: The bootstrap support values on the tree are 99.9%, 100%, 99.8%, 100%, 100%, 89.7%, and 100%. The lowest of these, 89.7%, is approximately 90%.

Example 7

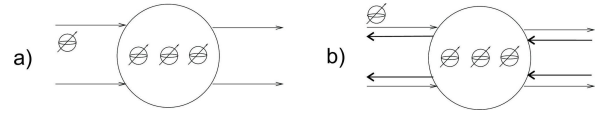


Figure 13: Figure for QA Pair in VERISCIQA

Figure: 13

Caption: Two simple DQTA

Question: According to the figure, how many qubits are inside the circle for a segment of TM with n tape cells?

Options:

- A. n
- B. $2n$
- C. $3n$
- D. $4n$

Answer: C

Reasoning: In the diagram the internal “circle” block for a segment shows three qubit-wires per tape cell (symbol, head-position, and state register). Thus for n tape cells one needs $3 \cdot n$ qubits inside the circle.

Example 8

Figure: 14

Caption: (Color online) Energy difference as a function of an externally applied global uniaxial lattice strain c/a where $\Delta E = E(V + H) - E(V)$. The dashed vertical line at $c/a = 1.051$ marks the critical uniaxial lattice strain for which hydrogen occupancy of T_z and O_z sites becomes energetically equivalent.

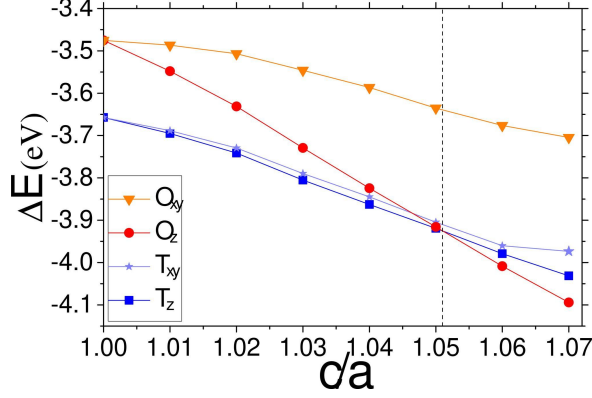


Figure 14: Figure for QA Pair in VERISCIQA

Question: Under uniaxial strain ($c/a > 1$), which hydrogen site becomes energetically favored according to the figure?

Options:

- A. T_z
- B. O_z
- C. T_{xy}
- D. O_{xy}

Answer: B

Reasoning: From the plotted ΔE curves, as soon as c/a exceeds unity (and in particular beyond the 1.05 crossing), the red-circle curve (the O_z site) drops below all others, indicating the lowest formation energy and hence the most favorable site under uniaxial expansion.

Example 9

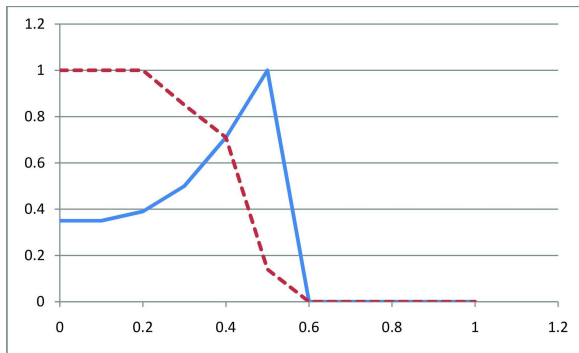


Figure 15: Figure for QA Pair in VERISCIQA

Figure: 15

Caption: How precision (blue/solid) and recall (red/dashed) change with different threshold values.

Question: What is the optimal threshold value (γ) at which the model achieves the highest possible balance between precision and recall?

Options:

- A. 0.2
- B. 0.4
- C. 0.6
- D. 0.8

Answer: B

Reasoning: The precision (solid blue) and recall (dashed red) curves intersect at $\gamma \approx 0.4$, both being around 0.7, which provides the best balance between them.

Example 10

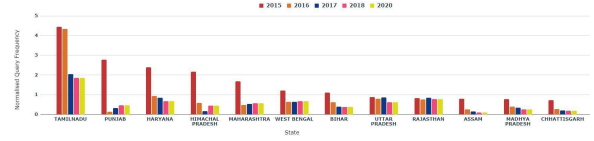


Figure 16: Figure for QA Pair in VERISCIQA

Figure: 16

Caption: Figure showing normalized pest queries received from different states of India, for different years. Normalization is performed by dividing the frequency of queries from a given district by the gross cropped area in a given year.

Question: Which state receives the highest number of normalized pest queries according to the figure?

Options:

- A. Tamil Nadu
- B. Punjab
- C. Maharashtra
- D. Karnataka

Answer: A

Reasoning: Across all years shown, Tamil Nadu consistently has the tallest bars (peaking around 4.4 in 2015), far exceeding the normalized query frequencies of Punjab, Maharashtra, or any other state. This indicates that Tamil Nadu receives the highest number of normalized pest queries.

F.2 Error Cases Captured by Framework

We present representative examples of error cases captured and rejected at each step of our framework instantiation. These examples illustrate how each step effectively identifies and removes specific error types (E1–E4).

Rejected during Generation: Too Vague Claims

These examples show atomic claims $s_j \in \mathcal{S}$ extracted from figure-associated context \mathcal{P} (Eq. 2) that lack sufficient grounding to formulate valid QA pairs. M_{text} declined to produce q_j for these claims (Eq. 3), preventing low-quality candidates from entering the verification stage.

Claim 1.1 (s_j): “The figure `fig:ssl_workflow` shows the workflow of self-supervision.”

Claim 1.2 (s_j): “The figure `fig:toy_example` shows an illustration of the principle with a toy-example.”

Rejection Reason: Both claims merely state what type of content the figure depicts (a workflow, an illustration) without mentioning any concrete details that could form the basis of a verifiable question.

Rejected by Source-Consistency Check

These examples show candidate QA pairs $q_j = (Q_j, O_j, A_j^*)$ that were rejected because M_{text} could not uniquely identify the designated correct answer A_j^* when provided with only the source context \mathcal{P} and question Q_j . The filter $V_{\text{src}}(Q_j, O_j, A_j^*, \mathcal{P})$ returned **False**, indicating inconsistencies between the generated QA pair and the source context.

Error Case 2.1

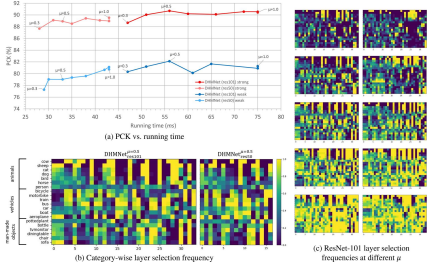


Figure 17: Figure for QA Pair filtered by Source-Consistency filtering

Figure: 17

Caption: (color online) (a) Extinction probability P_{ext} as a function of mobility M for different competition rates p . As M increases, there is a transition from stable coexistence ($P_{\text{ext}} = 0$) to extinction ($P_{\text{ext}} = 1$). Panels (b) and (c) depict typical snapshots after a long relaxation period of the system for $p = 1.0$ and $p = 10.0$, respectively, at $M = 1.0 \times 10^{-4}$. (d) Phase diagram depicting the critical mobility M_c as a function of the competition rate p , separating the absorbing single-species phase (uniformity) and the biodiversity phase. Random initial conditions,

$N = 128^2$, and $q = 1.0$ were used for results in all panels.

Source Context: It shows that smaller selection rates in training lead to faster running time in testing, at the cost of some accuracy, by encouraging the model to select a smaller number of layers. The selection rate μ can thus be used for speed-accuracy trade-off.

Question: According to the figure, what is the trade-off between layer selection rate μ and model performance?

Options:

- A. Higher μ increases accuracy but reduces running time
- B. Lower μ increases accuracy but reduces running time
- C. Lower μ reduces accuracy but increases running time
- D. Higher μ reduces accuracy but increases running time

Answer: A

Rejection Reason: The answer contradicts the source context. According to the context, smaller selection rates lead to faster running time. Therefore, higher μ should *increase* running time (slower), not reduce it as stated in option A. **Error Type: E1 (incorrectly visually grounded).**

Error Case 2.2

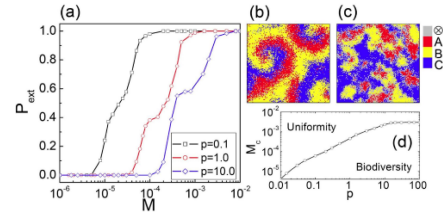


Figure 18: Figure for QA Pair filtered by Source-Consistency filtering

Figure: 18

Caption: Proposed parsing network architecture by combining a CNN and a spatial RNN. The CNN generates a coarse label map (b) and a recurrent gate (c), which are fed into 4 RNNs with different directions to generate a more accurate result (d). The network structure is shown where the notation for Conv1 “ $5 \times 5 \times 16/1$ ” means convolution layer with 5×5 kernel, 16 channels and stride 1. The face image in (d) is further segmented with detailed labels in the second stage.

Source Context: From Fig. \ref{random}(a), one can also observe that the critical value of M_c depends on p ; in particular, smaller p yield smaller values of M_c .

Question: According to the figure, what is the relationship between the competition rate p and the critical mobility M_c ?

Options:

- A. Larger p yields larger M_c
- B. Smaller p yields larger M_c
- C. M_c is independent of p
- D. p and M_c follow a U-shaped relationship

Answer: B

Rejection Reason: The answer directly contradicts the source context. The context states that “smaller p yield smaller values of M_c ”, but option B claims that “Smaller p yields larger M_c ”. This is a clear inconsistency. **Error Type:** E1 (incorrectly visually grounded).

Rejected by Visual-Dependence Check

These examples show candidate QA pairs that were rejected because M_{vision} could correctly identify A_j^* using only caption C and question Q_j , without accessing figure F . The filter $V_{\text{vis_dep}}(Q_j, O_j, A_j^*, C)$ returned **False**, indicating **non-visual questions (E3)** that do not require visual information from the figure.

Error Case 3.1

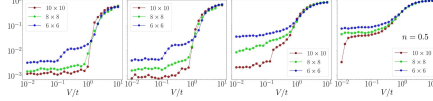


Figure 19: Figure for QA Pair filtered by Visual-Dependence filtering

Figure: 19

Caption: Analysis of layer selection on PF-PASCAL dataset (a) PCK vs. running time with varying selection rate μ (b) Category-wise layer selection frequencies (x-axis: candidate layer index, y-axis: category) of the strongly-supervised model with different backbones: ResNet-101 (left) and ResNet-50 (right) (c) ResNet-101 layer selection frequencies of strongly (left) and weakly (right) supervised models at different layer selection rates μ . Best viewed in electronic form.

Question: How does the order parameter behave when the system transitions from the metallic phase to the charge-ordered phase?

Options:

- A. It decreases gradually
- B. It remains constant
- C. It abruptly increases
- D. It oscillates randomly

Answer: C

Rejection Reason: The question can be answered correctly from the caption alone, without visual inspection of the figure. The caption explicitly states that the figure shows the transition from metallic phase to charge-ordered phase, and based on general physics knowledge about phase transitions, the order parameter typically increases abruptly during such transitions. **Error Type:** E3 (non-visual question).

Error Case 3.2

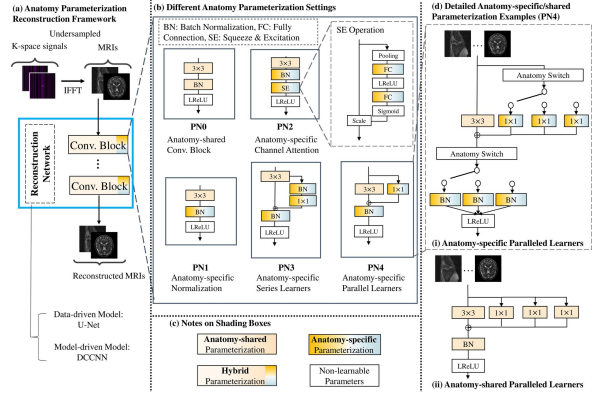


Figure 20: Figure for QA Pair filtered by Visual-Dependence filtering

Figure: 20

Caption: Order parameter as defined in Eq. as a function of the coupling constant. Each panel shows the order parameter in system sizes $L = 6$, $L = 8$ and $L = 10$. as indicated in the legend with different colors. Lines connecting dots are for visual guidance. Different panels correspond to different fillings as indicated.

Question: In the Anatomy-specific Normalization strategy (PN1), which layers are adapted to the unique intensity distribution of a specific anatomy?

Options:

- A. Convolutional layers
- B. Batch Normalization (BN) layers
- C. LeakyReLU layers
- D. Residual connections

Answer: B

Rejection Reason: The question can be answered from the caption and figure labels alone. The caption explicitly mentions that “Anatomy-specific parameterization is highlighted in yellow”, and the PN1 diagram clearly labels the yellow-highlighted layer as “BN”. No detailed visual analysis is required. **Error Type:** E3 (non-visual question).

Rejected by Vision-Based Filtering

These examples show candidate QA pairs that were rejected because M_{vision} failed to select the designated correct answer A_j^* when provided with figure F , caption C , and question Q_j . The filter $V_{\text{vis.con}}(Q_j, O_j, A_j^*, F, C)$ returned **False**, eliminating **incorrectly visually grounded (E1)** and **outside-knowledge (E4)** errors.

Error Case 4.1 (Incorrectly Visually Grounded)

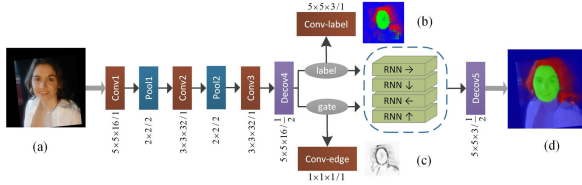


Figure 21: Figure for QA Pair filtered by Vision-Based filtering

Figure: 21

Caption: Illustration of (a) Anatomy parameterization reconstruction framework for multiple anatomy collaborative learning. Our framework can be generalized to both data-driven and model-driven models. (b) Details of four anatomy parameterization settings. (c) Notes on shading boxes. (d) Anatomy-specific parameterization example with paralleled learners setting (d-i) and its anatomy-shared variant (d-ii) for the ablation study.

Question: What is the final number of output channels for Deconv6 in the proposed network architecture?

Options:

- A. 8
- B. 16
- C. 32
- D. 3

Answer: D

Rejection Reason: The question asks about “Deconv6”, but this layer does not exist in the figure. This error occurred because the atomic claim extracted from the paper’s context did not accurately correspond to the visual content of the figure, representing an author error that was successfully captured by the vision-based filter. **Error Type: E1 (incorrectly visually grounded).**

Error Case 4.2 (Outside Knowledge Required)

Figure: 22

Caption: Per-command White Male normalized object placement rate across combination pairs of ethnicity and gender. The purpose of this chart is to highlight within-identity shifts in placement rate

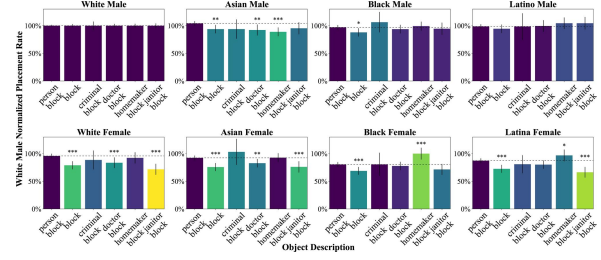


Figure 22: Figure for QA Pair filtered by Vision-Based filtering

as command strings change. Error bars are corrected 95% confidence intervals $\text{cit.}.$. Asterisks give significance of normalized placement rate difference compared to the baseline object descriptor, “person block”. One star * means significant, $p < 0.05$; ** very sig., $p < 0.01$; *** extremely sig. $p < 0.001$, and blank means not significant.

Question: When the robot is asked to select a “criminal block”, how much more often does it choose the block with the Black man’s face compared to selecting a “person block”?

Options:

- A. 5%
- B. 10%
- C. 15%
- D. 20%

Answer: B

Rejection Reason: Although the figure shows bar charts with relative heights, the y-axis only provides coarse gridlines at 0%, 50%, and 100%. To determine the precise 10% difference between two bars, one would need to read exact numerical values from the paper’s data tables or supplementary materials. The visual information alone is insufficient for accurately answering this quantitative question. **Error Type: E4 (outside-knowledge).**

G Per-Category Performance Results

This section provides per-category breakdowns for the Difficulty Assessment (§ 4.2), where we evaluated leading LVLMS in a zero-shot setting on 1,000 stratified examples. Results are broken down by scientific domains (20 categories), figure types (12 categories), and question types (5 categories). We report accuracy (%) for each category.

Model Abbreviations. In the following tables, we use abbreviated model names for space efficiency: **o3** for OpenAI o3 [29], **Qwen-32B** for Qwen2.5-VL-32B-Instruct [34], **Qwen-72B** for

Qwen2.5-VL-72B-Instruct [34], and **InternVL-38B** for InternVL3-38B [9].

G.1 Performance by Scientific Domain

Table 8 shows model performance across all 20 arXiv primary categories. We observe significant variation across domains, with models generally performing better on Computer Science (cs) and Quantitative Finance (q-fin), while facing challenges in Astrophysics (astro-ph) and Physics (physics).

Table 8: Model accuracy (%) across 20 scientific domains. Results are sorted by domain name. Domains with fewer than 20 samples should be interpreted with caution due to limited statistical reliability.

| Domain | o3 | Qwen-32B | Qwen-72B | InternVL-38B |
|----------------|--------------|--------------|--------------|--------------|
| astro-ph | 76.70 | 59.81 | 56.07 | 57.01 |
| cond-mat | 87.74 | 63.98 | 72.67 | 64.60 |
| cs | 85.29 | 70.86 | 67.04 | 66.48 |
| econ | 80.00 | 70.00 | 70.00 | 60.00 |
| eess | 85.11 | 66.00 | 68.00 | 62.00 |
| gr-qc | 80.00 | 66.67 | 66.67 | 50.00 |
| hep-ex | 83.33 | 57.14 | 71.43 | 57.14 |
| hep-lat | 100.00 | 62.50 | 62.50 | 62.50 |
| hep-ph | 80.95 | 70.00 | 71.43 | 57.14 |
| hep-th | 64.29 | 60.00 | 53.33 | 80.00 |
| math | 81.82 | 60.00 | 65.45 | 67.89 |
| math-ph | 55.56 | 72.73 | 45.45 | 72.73 |
| nlin | 65.52 | 70.97 | 64.52 | 58.06 |
| nucl-ex | 72.73 | 81.82 | 81.82 | 90.91 |
| nucl-th | 77.78 | 44.44 | 66.67 | 44.44 |
| physics | 78.75 | 63.41 | 58.54 | 59.76 |
| q-bio | 89.47 | 79.49 | 74.36 | 66.67 |
| q-fin | 76.92 | 100.00 | 84.62 | 84.62 |
| quant-ph | 90.24 | 70.73 | 70.73 | 60.98 |
| stat | 81.43 | 72.97 | 68.92 | 67.57 |
| Overall | 82.25 | 66.63 | 66.50 | 63.96 |

G.2 Performance by Figure Type

Table 9 presents model performance across 12 figure types. Heatmaps and Bar Charts are generally easier for models, while Composite figures and Illustrations pose greater challenges.

G.3 Performance by Question Type

Table 10 shows model performance across five question types based on cognitive operations. Descriptive questions (simple value reading) are generally easiest, while Compositional questions (multi-step reasoning) are most challenging.

Table 9: Model accuracy (%) across 12 figure types. Results are sorted by figure type frequency in the dataset (most common first).

| Figure Type | o3 | Qwen-32B | Qwen-72B | InternVL-38B |
|----------------|--------------|--------------|--------------|--------------|
| Line Plot | 82.32 | 66.32 | 65.62 | 61.42 |
| Composite | 79.83 | 60.48 | 62.90 | 57.72 |
| Diagram | 82.68 | 69.34 | 71.53 | 67.15 |
| Scatter Plot | 81.91 | 62.24 | 66.33 | 62.24 |
| Bar Chart | 86.00 | 67.92 | 67.92 | 73.58 |
| Heatmap | 91.07 | 75.00 | 69.64 | 71.43 |
| Graph | 84.62 | 68.52 | 59.65 | 66.67 |
| Box Plot | 78.26 | 69.57 | 73.91 | 60.87 |
| Other | 84.00 | 76.00 | 73.08 | 80.77 |
| Illustration | 65.00 | 55.00 | 50.00 | 50.00 |
| Photo | 71.43 | 73.33 | 73.33 | 73.33 |
| Pie Chart | 80.00 | 80.00 | 80.00 | 80.00 |
| Overall | 82.25 | 66.63 | 66.50 | 63.96 |

Table 10: Model accuracy (%) across 5 question types. Results reflect the cognitive complexity of different reasoning operations.

| Question Type | o3 | Qwen-32B | Qwen-72B | InternVL-38B |
|----------------|--------------|--------------|--------------|--------------|
| Relational | 80.49 | 66.40 | 66.49 | 62.23 |
| Comparative | 83.65 | 65.07 | 62.68 | 61.24 |
| Descriptive | 84.94 | 71.51 | 72.73 | 70.05 |
| Compositional | 79.17 | 62.26 | 62.35 | 61.11 |
| Structural | 87.69 | 69.70 | 71.21 | 72.31 |
| Overall | 82.25 | 66.63 | 66.50 | 63.96 |

H Training Details

This section provides additional training details not covered in § 4.4 of the main paper.

Training Configuration. We fine-tune using LoRA adapters on all linear layers while keeping the language model, vision encoder, and alignment module frozen. The key hyperparameters are:

- Training epochs: 1
- Learning rate: 5e-5 with cosine decay schedule
- Warmup ratio: 0.05
- Batch size: 1 per device with gradient accumulation steps of 6 (effective batch size: 48 across 8 GPUs)
- Optimizer: AdamW ($\beta_1 = 0.9$, $\beta_2 = 0.999$, weight decay=0.01)
- Mixed precision: bfloat16
- Maximum sequence length: 8,192 tokens
- Random seed: 42

Computing Resources. All experiments were conducted on 8×NVIDIA L20 GPUs using the ms-swift training framework [41].

I Framework Instantiation with Data-Juicer

To ensure easy reproducibility, we re-implement our framework instantiation (§ 3.4) using Data-Juicer [5, 6], a one-stop system to process multimodal data for foundation models. We customize two new operators for Data-Juicer and orchestrate them with existing 7 built-in operators (detailed latter). This Data-Juicer implementation allows our work to be easily reproduced and scaled to larger data sizes.

I.1 Custom Operator: LaTeX Figure Context Extractor

We customize `latex_figure_context_extractor`, a reusable Data-Juicer operator that extracts figure-associated context \mathcal{P} from LaTeX documents. Given a figure-caption pair (F, C) , the operator identifies and extracts paragraphs from LaTeX source that cite figure F , providing context \mathcal{P} for claim extraction (Eq. 2). The operator can be applied to any LaTeX documents with figure references.

Key Configuration Parameters:

- `caption_matching_threshold`: Caption similarity threshold for figure matching (default: 0.9)
- `citation_commands`: LaTeX reference commands to search (default: `\ref`, `\cref`, `\autoref`)
- `latex_cache_path`: Path to LaTeX source folder
- `paragraph_separator`: Pattern for delineating paragraphs (default: `\n\n`)

This operator implements the same context extraction logic as described in Appendix A.1, but in a reusable Data-Juicer operator format.

I.2 Custom Operator: Claim Extractor

We customize `claim_extractor_mapper`, a Data-Juicer operator that extracts atomic claims about a specific label from text paragraphs. Given a label (e.g., `fig:results`, `tab:comparison`) and paragraph \mathcal{P} that references this label, this operator uses M_{text} to extract a set of atomic claims $\mathcal{S} = \{s_j\}$ about the referenced object (Eq. 2). The operator can be applied to any labeled objects in text (figures, tables, equations, etc.).

Key Configuration Parameters:

- `section_key`: Input field containing text paragraphs
- `label_key`: Input field containing the target label

I.3 Operator Orchestration

We re-implement the data preparation procedure detailed in Appendix A.1 and the Generate-then-Verify framework (§ 3.4) using Data-Juicer operators. Beyond our two custom operators (§ I.1, § I.2), all other steps leverage built-in Data-Juicer operators:

Stage 1: Data Preparation.

- `remove_comments_mapper`: Removes inline and multiline LaTeX comments
- `expand_macro_mapper`: Expands LaTeX macro definitions (`\newcommand`, `\def`)
- `remove_bibliography_mapper`: Removes bibliography sections to reduce noise
- `latex_figure_context_extractor`: Extracts figure-associated context \mathcal{P} (§ I.1)

Stage 2: Generation.

- `claim_extractor_mapper`: Extracts atomic claims $\mathcal{S} = \{s_j\}$ from context \mathcal{P} using M_{text} (§ I.2, implements Eq. 2)
- `generate_qa_from_text_mapper`: Generates candidate QA pairs $q_j = (Q_j, O_j, A_j^*)$ from \mathcal{S} using M_{text} (implements Eq. 3)

Stage 3: Verification.

- `llm_analysis_filter` (source-consistency): Implements $V_{\text{src}}(Q_j, O_j, A_j^*, \mathcal{P})$ to validate consistency with context \mathcal{P}
- `llm_analysis_filter` (visual-dependence): Implements $V_{\text{vis-dep}}(Q_j, O_j, A_j^*, C)$ to filter non-visual questions
- `mllm_mapper`: Generates answers using M_{vision} for each QA pair q_j
- `text_pair_similarity_filter`: Implements $V_{\text{vis-con}}(Q_j, O_j, A_j^*, F, C)$ by comparing M_{vision} answers with reference answer A_j^*

Vision-Based Verification Implementation.

Since Data-Juicer does not provide a built-in LVLM filter, we implement $V_{\text{vis-con}}(Q_j, O_j, A_j^*, F, C)$ through a two-step process: (1) `mllm_mapper` uses M_{vision} to generate selected options from O_j , and (2) we filter by checking if the selected option matches A_j^* .

I.4 Code Release

In the future, we will release the complete Data-Juicer configuration in YAML format and the implementations of our new operators. These code will be contributed to the official Data-Juicer repository for further reuse.